Survey of recent advances of in the field of π-conjugated heterocyclic azomethines as materials with tuneable properties

ARTICLE *in* SCIENCE CHINA-CHEMISTRY · JANUARY 2012

Impact Factor: 1.7 · DOI: 10.1007/s11426-012-4778-4

3 AUTHORS, INCLUDING:

Andréanne Bolduc
Technische Universiteit Eindhoven
19 PUBLICATIONS **211** CITATIONS
SEE PROFILE

Charlotte Mallet
Hydro-Québec
19 PUBLICATIONS **115** CITATIONS
SEE PROFILE

SCIENCE CHINA
Chemistry

• REVIEWS •

doi: 10.1007/s11426-012-4778-4

Survey of recent advances of in the field of π-conjugated heterocyclic azomethines as materials with tuneable properties

BOLDUC Andréanne, MALLET Charlotte & SKENE W.G.*

Laboratoire de caractérisation photophysique des matériaux conjugués, Département de Chimie, Université de Montréal, CP 6128, Centre-ville, Montreal, QC H3C 3J7, Canada

Received June 19, 2012; accepted September 29, 2012

This account gives an overview of our recent work in the area of conjugated azomethines derived from 2-aminothiophenes. It will be presented that mild reaction conditions can be used to selectively prepare symmetric and unsymmetric conjugated azomethines. It further will be demonstrated that azomethines consisting of various 5-membered aryl heterocycles lead to chemically, reductively, hydrolytically, and oxidatively robust compounds. The optical and electrochemical properties of these materials can be tuned contingent on the degree of conjugation, type of aryl heterocycle, and by including various electronic groups. The end result is materials having colors spanning 250 nm across the visible spectrum. These colors further can be tuned via electrochemical or chemical doping. The resulting doped states have high color contrasts from their corresponding neutral states. The collective opto-electronic properties and the means to readily tune them, make thiophenoazomethine derivatives interesting materials for potential use in a gamut of applications.

review, azomethines, electronic *push-pull*, electrochromism, polymers, thiophene, conjugated materials, X-ray crystallography

1 Introduction

The awarding of the Nobel prize to Prof. A. Heeger, A. MacDiarmid, and H. Shirakawa in 2000 for their discovery and development of conductive polymers subsequently spurred a girth of research in the area of conjugated materials [1]. During the ensuing twenty years, many advances have occurred in both the preparation of π-conjugated materials and property enhancement [2–5]. Many strategies employed for materials preparation have been adopted from small molecule synthesis, including Suzuki-Miyaura [6], Yamamoto [7], Kumada-Corriu-Tamo [8], Stille [9], Grignard Metathesis [10] and Heck [11] coupling protocols, to iterate but a few [12]. Recently C–H activation has also successfully been applied towards preparing conjugated polymers with the advantage of affording higher molecular weight polymers than with conventional polymerization techniques [13]. The advantage of a wide range of coupling strategies available for preparing materials is that the electronic, optical, and electrochemical properties of the materials can be tailored. This results in conjugated π-systems whose opto-electronic properties are compatible for use in a wide range of plastic electronics. This is evidenced by the successful use of these materials in plastic devices including organic light emitting diodes [14–16], photovoltaic devices [17, 18], electrochromic devices [19, 20], organic field effect transistors [21], and recently light emitting field effect transistors [22, 23], with various devices being used in many consumer applications.

While a plethora of methods are available for preparing conjugated materials, most require stringent reaction conditions including inert atmospheres, anhydrous solvents, and expensive catalysts [24]. The resulting materials must further be purified extensively to remove residual catalysts,

*Corresponding author (email: w.skene@umontreal.ca)

ligands, and substantial amounts of by-products. The latter is particularly prevalent with vinylene (–CH=CH–) materials that are prepared from Horner-Emmons and Wittig protocols [25–28]. Azomethines (–N=CH–) are ideal alternatives to vinlyene materials in part owing to their isoelectronic character with their vinylene analogues [29]. Azomethines should exhibit similar opto-electronic properties to their all-carbon counterparts. Azomethines are also synthetically advantageous compared to their vinylene counterparts. This is in part owing to water being the unique by-product, which can readily be absorbed by using hygroscopic solvents for their preparation [30]. As a result, minimal purification is required for the isolation of azomethines, and stringent conditions are not required for their preparation.

Despite the synthetic and purification advantages of azomethines, they have been overlooked as viable alternatives for conjugated functional materials. This is in part a result of azomethines being assumed to readily hydrolyse and decompose. They are further understood not to possess opto-electronic properties that are suitable for their use in plastic devices. The focus of this review is therefore to present heterocyclic azomethines as viable functional materials having opto-electronic properties that are compatible for use in plastic devices. The objective is further to demonstrate that the opto-electronic properties of these conjugated and robust materials can readily be tailored contingent on structure. This review will not take into account azomethines used as coordinating ligands with metals. Instead, it will focus on 5-membered heterocyclic azomethine prepared uniquely from the 2-aminothiophenes **MAT** and **DAT** (Figure 1). Given the wealth of reports detailing azomethines, the focus will be limited to accounts spanning the past six years.

The organization of this review is as follows: a concise historical perspective of homoaryl azomethines and their uses will be presented followed by X-ray crystal structures of the few known examples of homoaryl azomethines. The collective data will allow the juxtaposition of their opto-electronic and crystallographic properties relative to their heterocyclic counterparts. Subsequently, the structure dependent opto-electronic and crystallographic properties of heterocyclic derivatives will be reviewed. It will be demonstrated that enhanced opto-electronic properties are possible with these heterocyclic derivatives. While the review focuses on small molecules, the concluding sections will briefly present the preparation and opto-electronic properties of heterocyclic polyazomethines, followed by future perspectives.

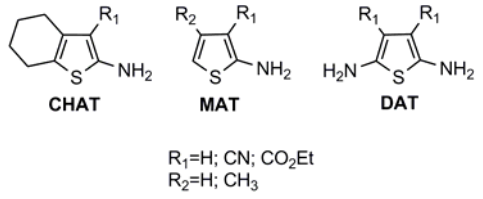

Figure 1 Examples of 2-aminothiophene derivatives detailed in this review.

2 Nomenclature and preparation

Azomethine, imine, and Schiff Base are synonymous and they represent the structure consisting of $R_1R_2C{=}NR_3$ (Figure 2). In the case of azomethines, R_3 is typically a substituent other than hydrogen. When R_3=H, the general term imine is applied. This class of heteroatomic bonds can further be divided into ketylimines and aldimines. Ketylmines consist of both R_1 and R_2 that are substituents other than hydrogen. Conversely, either R_1 or R_2 is a hydrogen for aldimines.

Aldimines are obtained from the condensation of an aldehyde and a primary amine as seen in Scheme 1. The reaction is reversible and the equilibrium can be shifted towards the products by the removal of water. Owing to their reversible formation and simple hydrolysis, in the case of unconjugated derivatives, Schiff bases have readily been used as protecting groups in synthetic organic chemistry. The complementarity of the amine and carbonyl groups for Schiff base formation is versatile in that the heteroatomic bond can be used to protect either an amine or a ketone. Displacing the equilibrium in favor of the desired azomethine can be done by azeotropic distillation using a Dean-Stark trap, molecular sieves, or hygroscopic solvents such as absolute ethanol or THF, for example. In certain cases, the product precipitates from the reaction mixture. This not only makes product isolation much easier, but it also prevents the product from being hydrolyzed [31].

Azomethine formation is typically catalyzed by a strong acid such as trifluoracetic acid (TFA). Lewis acids such as zinc chloride can also be used and titanium tetrachloride is often employed for preparing sterically hindered products. The disadvantage of using the latter for preparing azomethines is that it must be used in at least stoichiometric amounts. This leads to substantial titanium by-products that must be removed. Moreover, substantial amounts of acid are produced during the reaction from the hydrolysis of $TiCl_4$ by ambient trace amounts of water. An excess of an organic base is therefore required to prevent both undesired protonation of the amine reagent and product hydrolysis. The use of this extreme dehydrating reagent therefore requires stringent reaction condition in addition to extensive puri-

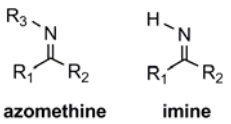

Figure 2 General structure of azomethines and imines.

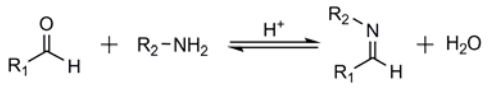

Scheme 1 General synthetic scheme for azomethine formation.

fication. This is in contrast to the use of TFA in conjunction with alcohol solvents, where the product is readily isolated upon either solvent removal or precipitation.

3 Brief historical perspective

The vast majority of reported conjugated azomethines have been prepared exclusively from either aniline or phenylene diamine (Figure 3). Their popularity is due to their high degree of stability and their widespread availability from commercial sources. This is in contrast to other aryl amines such as 2-substituted thiophenes that readily oxidize owing to their electron richness [32]. The resulting azomethines prepared from unstable arylamines are equally unstable and they either readily oxidize or hydrolyze. However, azomethines prepared from the 2-aminothiophene amines in Figure 3 were both resistant towards acid hydrolysis and reduction [33]. They additionally possessed high oxidation potentials making them extremely stable under ambient conditions and at high temperatures.

The isoelectronic character of the azomethine bond relative to its vinylene analogue was demonstrated by Jenekhe *et al.* who prepared poly(1,4-phenylenemethyldyenitrilo-1,4-phenylenenitromethylidyne) (**PPI**). The resulting polyazomethine (Figure 4) had similar spectroscopic and thermal properties to its all-carbon counterpart, poly(*p*-phenylene-vinylene) (**PPV**) [34]. The added advantage of **PPI** over **PPV** was that the azomethine derivative could be both oxidized and reduced, unlike **PPV** that could only be oxidized. Heteroatom containing materials therefore can be both p- and n-type materials. The polyazomethine was additionally more stable under ambient conditions than **PPV**. This was in part owing to its higher oxidation potential and larger energy gap. The difference in electrochemical properties was courtesy of the electronic withdrawing effect of the azomethine that increased both the HOMO and LUMO energy levels.

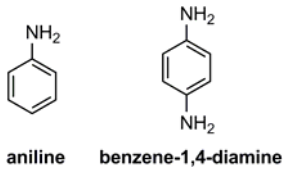

Figure 3 Homoaryl precursors commonly used for azomethine preparation.

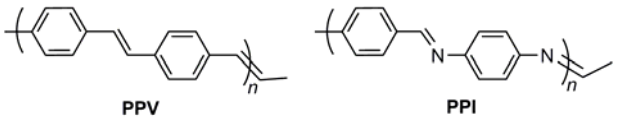

Figure 4 Examples of isoelectronic polymers.

3.1 Uses of conjugated azomethines

Materials derived from homoaryl azomethines have been used in various applications. These include applications in biology as fungicides [35–37], antimicrobials [38, 39], antiproliferatives [40] and enzyme inhibitors [41, 42], to name but a few. They have also been used in other biological applications to complex metals [43, 44]. Azomethines have found additional uses as polymer organic frameworks (POFs) for H_2 and CO_2 sequestering [45, 46]. This is a result of their large surface area [47, 48]. They have further been used as epoxy-derivatives for the preparation of thermostable and thermoconductive polymers [49–51]. The thermal stability of the azomethines is courtesy of the rigid imine bond. Their thermal stability and thermal conductivity have been exploited for use as electrical isolators and adhesives in motors, transformers and integrated circuits.

While azomethines are nonfluorescent because of intrinsic fluorescence quenching modes [52–54], efforts have been dedicated to selectively turn-on the fluorescence for sensor applications [55]. For example, Farcas *et al.* used a pyrene-triazole azomethine derivative in a rotaxane conformation for polymer encapsulation in cyclodextrine (CD) [56]. In the non-rotaxane conformation, the polymers were nonfluorescent. However, the fluorescence was enhanced with the addition of CD owing to confinement effects. Derinkuyu *et al.* also used azomethine dyes to investigate their fluorescence behavior as well as their pH-dependent fluorescence in common solvents and polymer matrices, such as polyvinylchloride (PVC) and ethyl cellulose (EC) [57]. They observed that the dyes were nonfluorescent in solution. In contrast, the azomethines exhibited high quantum yields in solid matrixes. This was ascribed to the suppression of inherent quenching mechanisms, such as vibrational deactivation when immobilized. Another example of fluorescence applications is from Liu *et al.* who covalently linked Schiff-base derivatives to an inorganic silica network for sol-gel applications and photoluminescence [58]. The azomethines similarly exhibited high fluorescence when they were immobilized in a sol-gel network. The underlying conclusion from these independent studies was that otherwise nonfluorescent azomethines could be rendered fluorescent by physically deactivating their inherent fluorescence quenching modes.

Azomethines have recently been used in plastic electronics such as photovoltaic devices, organic field effect transistors and electrochromic devices. For example, Sek *et al.* synthesized a series of triphenylamine (TPA) oligomers that are

normally used as hole-transporting materials in organic light emitting diodes [59]. They coupled TPA to various fused homoaryl amines. The resulting azomethines exhibited both high thermal stability and large energy gaps. Nonetheless, the TPA azomethine derivatives had hole-transport properties, illustrating the semi-conductive character of the imines. Triphenylamine azomethines were similarly used by Yen *et al.* to make electrochromic polymers [60]. Their polymers underwent two-step color changes with increasing applied potentials as result of radical cation and dication formation. The two species were reversibly generated and stable towards multiple switching between positive and negative applied potentials. The TPA azomethines switched between red and blue. Electrochromic azomethines were also demonstrated by Is *et al.* [61] who observed enhanced colors in both the neutral and oxidized intermediates. The observed color transitions were between orange and green when using an electron rich pyrrole-carbazole-pyrrole azomethine comonomer that was anodically polymerized onto transparent ITO electrodes. The resulting polymer immobilized on the electrode retained its optical activity even after a 1000 cycles of electrochemical switching.

Liquid crystals (LC) have additionally been prepared from azomethines. This is courtesy of the imine bonds that have a high propensity to undergo intermolecular π-stacking. The intrinsic crystalline behaviour was exploited to make various types of mesophase-like LCs. An example of azomethine LC formation is by Gao *et al.* who prepared liquid crystalline epoxy (LCE) resins. The azomethine LCE exhibited higher thermal properties and improved adhesive toughness, relative to normal LCEs [62]. Functionalizing the epoxy resin with azomethines also improved the mechanical properties without reducing the thermal resistance. Darla *et al.* similarly used azomethines for the preparation of thermally stable and thermotropic LCs for non-linear optics [63]. Their compounds showed enhanced non-linear optical properties over their corresponding all-carbon counterparts. Iwan *et al.* also prepared LCs by binding a polar spacer between two azomethine mesogens [64]. The LC exhibited optical, thermoluminescent, and current-voltage properties. It was found that the LCs became luminescent with increasing temperature. The LCs were successfully used as emitting materials in organic light emitting diodes with a turn-on voltage of 0.250 V. Iwan *et al.* further successfully demonstrated that opto-electronic properties compatible for plastic device usage were possible with aliphatic azomethine LCs [65]. Similarly, Hindson *et al.* prepared LCs from TPA for hole transporting layers in photovoltaic devices [66]. The effect of varying the exocyclic bond angle between the aromatic substituent connected to TPA on the thermal, optical and photoelectronic properties was studied. It was found that decreasing the azomethine exocyclic angle between TPA and various aromatics decreased the LC degree of conjugation. It was further found that the LCs were photoluminescent and they had low energy gaps in the order of 2.2 eV. The usefulness of these materials in plastic electronics was successfully demonstrated by preparing bulk heterojunction photovoltaic devices having power conversion efficiencies in the order of 0.1%. The collective examples illustrate that azomethines have functional materials-like properties. Moreover, they can successfully be used in devices in part owing to the inherent properties of the –N=CH– bond and its robustness.

3.2 Crystallographic structures of homoaryl azomethines

Given their high propensity to form LCs, it is surprising that there is little crystallographic data available for homoaryl azomethine derivatives. One of the first reported X-ray structures was by Bürgi *et al.* who solved the structures of (*E*)-*N*-benzylideneaniline (Figure 5) and its 4-substituted derivatives [67]. The azomethines all crystalized in the $P2_1/c$ group having 4 molecules per lattice. The striking features of the crystals were the azomethine isomer that was adopted and the coplanarity of the benzenes and the azomethine. In all cases, the thermodynamically stable *E* isomer was resolved. This is of importance given that the absolute configuration of the isomer cannot unequivocally be resolved by other standard characterization techniques. The crystallographic data further showed that the angle between the mean planes described by the azomethine and the phenyl adjacent to the =CH was consistently ca. 50°. The twisting from coplanarity is a result of interactions between the benzene's *ortho* hydrogens and that of the azomethine. The large twist angle between the aryl-azomethine planes limits the degree of conjugation of arylazomethines. This is evident in both their hypsochromic spectroscopic properties and higher oxidation potentials relative to their vinylene counterparts, which are coplanar (3.4°) and have higher degrees of conjugation [68, 69]. Azomethines can be made coplanar with the aromatics to which they are connected by

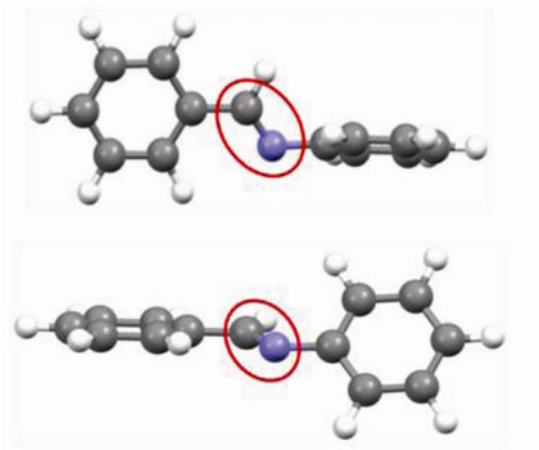

Figure 5 Face (top) and edge (bottom) view of the X-ray crystal structure of (*E*)-*N*-benzylideneaniline illustrating the twist from coplanarity of the aryl-azomethine planes. The azomethine bond is highlighted for clarity.

replacing the 6-membered homoaryls with 5-membered aromatics (*vide infra*). The twisting angle can additionally be reduced with 6-membered aromatics by using derivatives with *ortho* substituents that have minimal interactions with the azomethine hydrogen. This is the case with pentafluorobenzene whose shorter C–F bonds lower the aryl-azomethine torsion angle to 36° [70, 71].

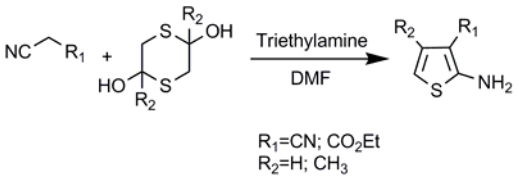

Scheme 2 Synthetic scheme for the general synthesis of **MAT**.

3.3 Aminothiophene derivatives

Thiophene derivatives have extensively been used in conjugated materials. This is in part owing to their interesting optical and electronic properties that are compatible for use in many applications [72]. Thiophene derivatives further possess good thermal and chemical stability. They also can be easily functionalized to adjust their optical and electrochemical properties in addition to their solubility. Most importantly, thiophenes have a low oxidation potential allowing them to be anodically polymerized at relatively low oxidation potentials. Similarly, their polymeric counterparts have high environmental stability in both their doped and undoped states. They further have high color contrast ratios between their neutral and doped states. These are ideal for electrochromic applications. Polythiophenes have additional interesting electronic properties. They are highly conductive when doped with conductivities on the order of 10^3 S cm^{-1} [73]. The collective semi-conductor properties of polythiophenes have led to their successful use in plastic electronic applications such as organic field effect transistors (OFETs) [74, 75], organic light emitting diodes (OLEDs) [76], photovoltaic devices and electrochromic devices [77, 78].

Thiophene azomethine derivatives should possess interesting opto-electronic properties along with enhanced opto-electronic properties compared to their homoaryl azomethine counterparts. Based on the crystallographic data of the homoaryl azomethines, thiophene azomethines are expected to have reduced torsion angles between the thiophene and azomethine planes (see crystallographic section). This would lead to highly extended π-conjugated systems with strong absorbances in the visible spectrum and electrochemical properties that are suitable for using the materials in electronic applications. While the required thiophene aldehyde is stable and can be reacted to form azomethines, its complementary aminothiophene is extremely unstable. Both 2-amino and 2,5-diaminothiophenes that are unsubstituted in their 3- and 4-positions are unstable and they spontaneously oxidize [32]. Owing to their extreme reactivity, there are only a few reported thiophene azomethines prepared from 2-aminothiophene [79–81].

Stable 2-aminothiophenes, such as those shown in Figure 1 would be beneficial for preparing all-thiophene azomethines. Such derivatives are possible by incorporating electron withdrawing groups in the α-position to the amine. The electron withdrawing group increases the oxidation potential making the 2-amino-3-substituted thiophenes less prone to oxidation under ambient conditions. Typically, aminothiophene derivatives are air stable and they can be prepared via the Gewald reaction [82–84]. In the case of 2-aminothiophenes, their preparation is done with activated methylenes, such as ethyl cyanoacetate or malononitrile in the presence of 1,4-dithiane-2,5-diol under basic conditions (Scheme 2) [45, 48]. 2-Aminothiophene derivatives such as CHAT are similarly prepared by replacing the activated methylenes with a ketone and proceeding via a Knoevenagel condensation. Given that the products can be handled under ambient conditions, their preparation is appropriate to large scale preparation. The products can also be readily isolated by either column chromatography or precipitation. The resulting R_1 group can further be modified, resulting in a wide range of stable 2-aminothiophene derivatives.

Similarly, stable 2,5-diaminothiophenes can be prepared via the Gewald reaction using activated methylenes and elemental sulfur (Scheme 3) [85–89]. In contrast to **MAT**, extensive purification of **DAT** is required to remove unreacted sulfur and sulfur derivatives. As a result, the product yield is poor. Nonetheless, the functional groups in the 3,4-position can be further reacted to provide a broad array of hydrophilic and hydrophobic stable 2,5-diaminothiophenes for various uses. Alternatively, the inexpensive cyanoacetic acid reagent can easily be esterified prior to the Gewald reaction to obtain a gamut of 2,5-diamino-thiophenes ester derivatives.

The stability of **MAT** and its derivatives is epitomized by their tolerance towards degradation when subjected to chemical modification. Any of the positions can be reacted without risk of decomposing the thiophene. The robustness of **MAT** and its derivatives has been exploited for preparing many biologically and pharmaceutically active 2-aminothiophenes for uses such as LIMK1 enzyme inhibitors against Williams syndrome [90–92], MNN enzyme inhibitors against leukemia [93] and adenosine A1 receptor antagonists [94–96]. **MAT** derivatives are also potent antimicrobials [97, 98] and fungicides [99].

The robustness of **MAT** has also been exploited to prepare various azo dyes (Figure 6) [100–108]. The 2-amino-

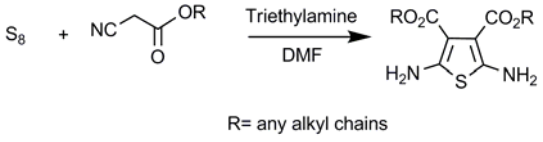

Scheme 3 Synthetic scheme for the general synthesis of **DAT**.

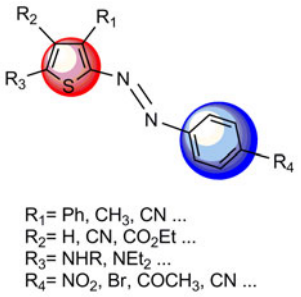

Figure 6 Various azo dyes prepared from MAT derivatives.

thiophene derivatives were found to withstand the harsh diazotisation reaction conditions. The generated diazonium intermediates were successfully coupled with various aromatics to afford stable azo dyes. A wide range of colors was possible by incorporating various electronic groups into the 3, 4, and 5-positions of **MAT** in addition to the *para*-position of the coupled aromatics. These dyes exhibited high colorfastness as well as resistance to bleaching, oxidation, and degradation.

4 Thiophene azomethine derivatives

MAT derivatives have been known for over 40 years [86, 87]. They have subsequently been examined extensively and they have been subjected to many modifications for biological, pharmaceutical, and dye-stuff uses. **DAT** was discovered approximately at the same time as its 2-monoamino counterpart. Interestingly, **DAT** and its derivatives have received limited attention and they have not been exploited to the full extent as their 2-monoamino counterparts. This is not a result of differences in stability or reactivity between **DAT** and **MAT**. Rather, the symmetry of **DAT** precludes structural modification for preparing pharmaceutically and biologically active interesting compounds. Nonetheless, polymers derived from 2,5-thiophene-3,4-dicarbonitrile have been prepared from the condensation with terephthalic dicarboxaldehyde [109–111]. These polymers were found to coordinate metals via the azomethine sites and the resulting metallo-polymer complexes were somewhat conductive, on the order of 1×10^{-4} S cm^{-1}.

Despite the abundant number of reports describing the synthesis and uses of **MAT**, its use in preparing π-conjugated azomethines, notably those consisting uniquely of thiophenes, were unknown until 2006 [112, 113]. Similarly, highly π-conjugated azomethines prepared from **DAT** were also unreported. We were therefore motivated to prepare conjugated thiophenes from 2-aminothiophene derivatives and to investigate their opto-electronic properties. Motivation was not only to demonstrate that such derivatives could be prepared, but to show that all-thiophene azomethines also exhibited interesting spectroscopic and electrochemical properties. It was anticipated that 5-membered heterocycles would minimize any interaction between the *ortho*-substitution and the azomethine hydrogen (see the crystallographic section). This would result in a highly coplanar arrangement of the aryl groups with the azomethine, leading to increased degrees of conjugation relative to its 6-membered counterparts. The added advantage of using thiophenes and other heterocycles is their electron richness. The high degree of conjugation of the 5-membered azomethines would promote extended delocalization of the electron rich heterocycles. This was expected to result in azomethines having strong absorbances in the visible and low oxidation potentials. Owing to the extended delocalization, it was also expected that the color of the azomethines could be tailored by incorporating various electronic groups, similar to their carbon counterparts [114, 115]. Readily tailoring the optical and electronic properties would make the azomethines amenable to meet the requirements for a wide range of applications. The extended degree of conjugation and expected bold visible color of the azomethines would be ideal for many spectroscopic applications including electrochromic and photovoltaic devices. Meanwhile, the highly ordered intermolecular packing arrangements observed with the homoaryl azomethines, taken together with their extended π-conjugation, would make thiophene azomethines suitable candidates for use in organic field effect transistors. Given the absence of reports relating to all-thiophene azomethines and their expected enhanced properties relative to their homorayl counterparts, we endeavored to prepare and characterize such derivatives. Subsequently, we have prepared and characterized the opto-electronic and crystallographic properties of many interesting conjugated azomethines derived from **DAT** and **MAT**. The ensuing sections will be devoted to surveying our recent advances relating to azomethines consisting of 5-membered heterocycles, spanning back to 2007. Focus will be placed on the property tuning, notably spectroscopic and electrochemical properties, contingent on the structure of the azomethine small molecules.

4.1 Synthesis

Conjugated polyazomethines possess interesting properties owing to their high degree of conjugation. They are also beneficial in terms of spectroscopic, electrochemical, mechanical, and thin film forming properties. However, accurate structure-property studies are challenging with polymeric systems. Therefore, we originally endeavored to study small molecules as viable model systems for examining the properties of all-thiophene azomethines. These provided the means for accurate property-structure assessment. The added advantage of small molecules is their reduced degree of conjugation relative to polymers, although they should be more susceptible to hydrolysis, decomposition, and reduction. The stability of the azomethine bond towards

acid hydrolysis and reduction could accurately be examined with small molecules.

Our original target was the all-thiophene derivative **4** (Scheme 4 and Figure 7). It was chosen as a model compound for examining the reaction conditions required for its preparation. It was also chosen to assess its stability under ambient conditions and its resistance towards acid hydrolysis and reduction. **4** was also expected to provide pivotal information relating to the spectroscopic and electrochemical properties of the novel azomethines.

Given that azomethines produce environmentally benign water as a by-product, they can be considered as environmentally friendly materials. However, their preparation according to conventional methods is not green. This is because many known methods for azomethine preparation require stringent reaction conditions and hygroscopic Lewis acids [116]. Their preparation also produces significant by-products that require extensive product purification. We therefore endeavoured to prepare **4** using mild reaction conditions that were consistent with an environmentally friendly approach, such as innocuous solvents and mineral acids, while avoiding the use of inert atmospheres. This approach would reduce the amount of by-products and potentially eliminate the need for product purification. A simple and straightforward preparation of azomethines would additionally make them interesting alternatives to their all-carbon counterparts, providing they exhibited similar spectroscopic and electrochemical properties.

Preliminary attempts to prepare **4** in ethanol using catalytic amounts of TFA consistently and exclusively led to the dyad **2**. The desired triad **4** was not formed even with a large excess of the aldehyde. The lack of formation of the desired product was a result of reduced reactivity of the terminal amine of **2**. This was owing to the electron withdrawing effect of the azomethine. The product could be formed using $TiCl_4$, however, it also could be prepared with mild conditions using alcohol solvents having high boiling points, such as *iso*-propanol and *n*-butanol. Alternatively, **4** could be prepared in the absence of solvent. Using exactly two equivalents of the aldehyde, **4** could be quantitatively obtained by melting the reagents in the presence of TFA vapor. The variable reactivity in different solvents was exploited to prepare unsymmetric triads in one-pot, according to Scheme 4. This was possible by using one equivalent of the first aldehyde and refluxing in ethanol. The resulting dyad was obtained quantitatively upon removing the solvent and it did not require purification. It was then redissolved in either *n*-butanol or *iso*-propanol in addition to one equivalent of a different aldehyde.

Azomethines are assumed to be hydrolytically unstable and they are known to be reduced with common reductants. Both the hydrolytic and reductive stability of **4** were subsequently investigated. It was found that **4** failed to hydrolyze in refluxing moist organic solvents in the presence of various acids even after prolonged reaction conditions. These conditions were chosen since they normally hydrolyze azomethines. **4** could further be purified by column chromatography using silica gel. The absence of decomposition of **4** with the inherent acid silica gel further demonstrated the resistance of conjugated azomethine to hydrolysis. The tolerance of **4** to reductants was additionally investigated using common reductants such as $NaBH_4$, $LiAlH_4$, and DIBAL [117]. No reduction or decomposition was observed either spectroscopically or by NMR. In fact, the characteristic imine proton at 8 ppm disappeared only after 24 hours under refluxing conditions with an excess of DIBAL. The collective results demonstrated the robustness of **4** and that it does not readily decompose, hydrolyze, or reduce.

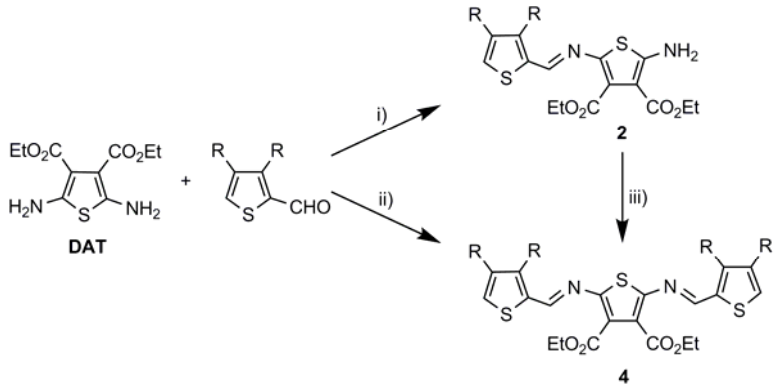

Scheme 4 Synthetic scheme illustrating the selective formation of azomethines prepared from **DAT**: (i) cat. TFA, EtOH; (ii) cat. TFA, *n*-BuOH or $TiCl_4$, DABCO, toluene; (iii) cat. TFA and either *n*-BuOH or *i*-PrOH.

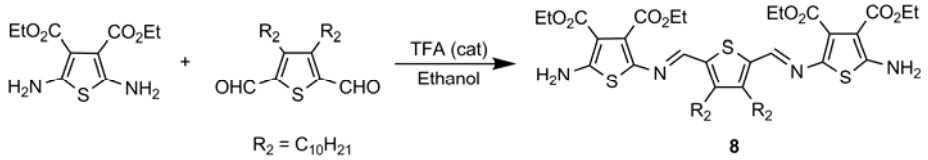

Scheme 5 General synthetic scheme of oligomer formation.

Scheme 4 illustrates that stoichiometry of the monoaldehydes and **DAT** is important for the selective formation of azomethines. Stoichiometry is equally important for selective product formation when condensing **DAT** with thiophene dialdehydes. Polymers having M_n on the order of 15 kg/mol were obtained with a 1:1 ratio of the reagents using specific reaction conditions (*vide infra*). Meanwhile, a 2:1 ratio of **DAT**/dialdehyde exclusively afforded triad **8** (Scheme 5). Unlike with **4**, **8** could be quantitatively obtained using mild reaction conditions such as ethanol with catalytic TFA at room temperature. **8** was also hydrolytically and reductively robust and air stable. The advantage of **8** over **4** is that it precipitated from solution and it could be quantitatively obtained without purification.

4.2 Effect of conjugation on optical properties

The successful preparation of **4** and **8** confirmed that the all-thiophene conjugated azomethines were stable. While the spectroscopic properties of **4** and **8** were similar and differed only by 64 nm, it was hypothesized that the spectroscopic properties could be tailored by varying the degree of conjugation. The derivatives illustrated in Figure 7 were therefore prepared for structure-property studies. Specifically, the azomethine placement and the effect of the degree of conjugation including the number of thiophenes (**1–7**) and the number of azomethines (**8–10**) on the optical and electrochemical properties were of interest. The compounds prepared were subsequently characterized by absorbance, fluorescence, and cyclic voltammetry.

The absorbance spectra showed that subtle changes to the azomethine structure significantly impacted the color. While **1** and **2** possessed a single azomethine, their absorbances were different. The absorbance of **2** was bathochromically shifted by 30 nm relative to **1**. The variation was a result of the electron donating effect of the terminal amine **2**, which reduced the energy gap. The same bathochromic trend was observed for all the azomethines having a terminal amine relative to those terminated with a hydrogen. The variation in absorbance induced by a slight structural modification was further obvious with **4** and **5**. The two azomethines differed only by alkyl groups in the 3,4-positions of the thiophene. The weak electron donating effect of the alkyl substituents reduced the energy gap, resulting in a 65 nm bathochromic shift.

The effect of the degree of conjugation and the number of thiophenes on the optical properties is obvious in Figure 8. The absorbance was bathochromically shifted by 66 nm when adding a thiophene upon going from **2** to **3**. However, the shift was less pronounced with additional thiophenes. A blue shift was observed between **3** and **4**, indicating that the terminal amine contributed more to the conjugation than a thiophene. However, there was still a small red shift of 4 nm between **3** and **6** and a 22 nm shift between **6** and **7**. The absorbance was less pronounced with the bithiophenes derivatives. This was in part owing to the reduced conjugation as a result of twisting between the bithiophenes. This was confirmed by the crystallographic data of **6** [118]. Nonetheless, the absorbance could be tailored over a range of 92 nm by structurally modifying the azomethines by including bithiophenes.

The impact on the absorbance was more pronounced with increasing the number of azomethines than with thio-

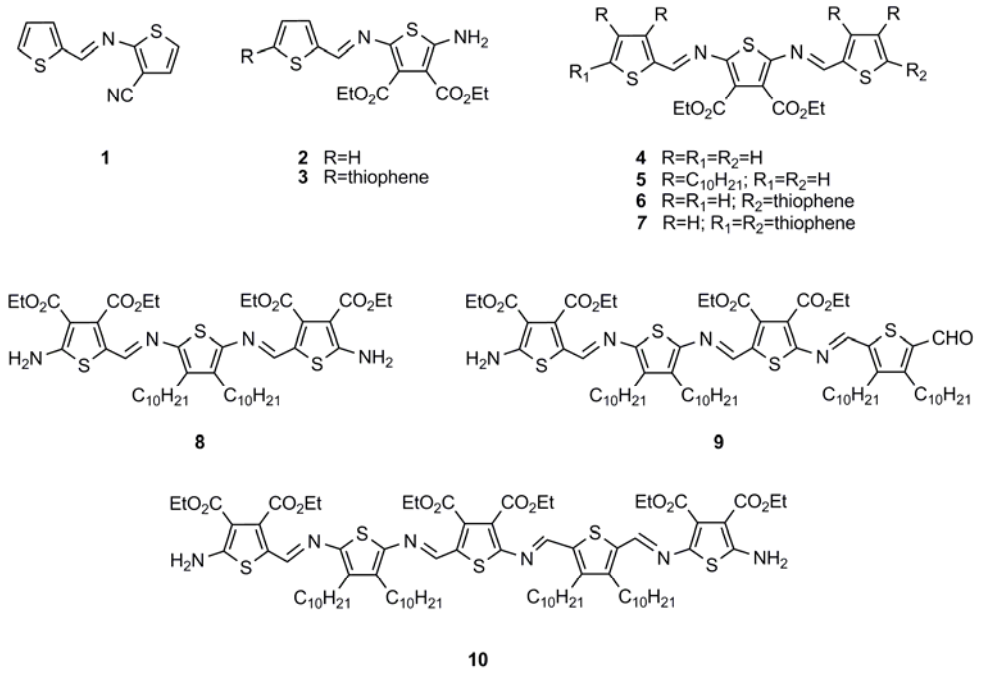

Figure 7 Azomethines prepared for examining the effect of degree of conjugation on the opto-electronic properties.

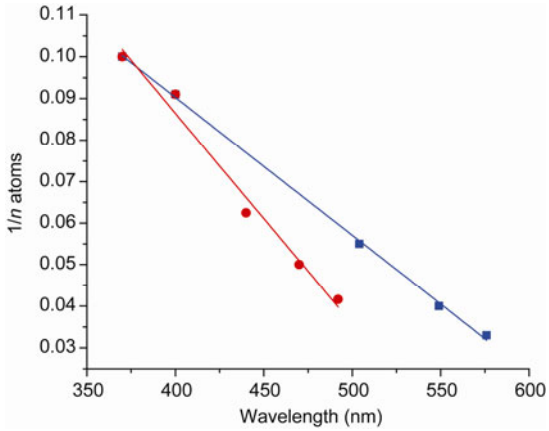

Figure 8 Effect of varying the number of azomethines (■) and thiophenes (●) on the absorbance maximum of the azomethines in Figure 7.

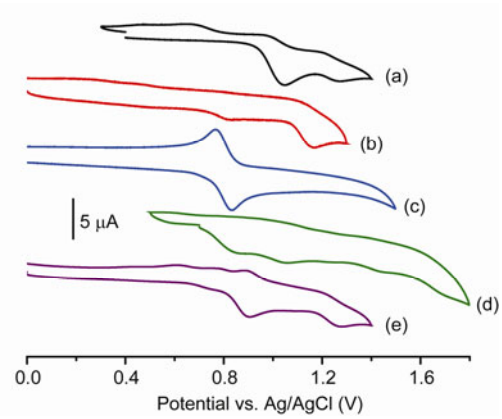

Figure 9 Anodic cyclic voltammograms of **2** (a), **4** (b), **8** (c), **9** (d) and **10** (e).

phenes. This is evident in Figure 8 that shows the change in wavelength as a function of the reciprocal number of atoms found along the conjugated backbone. A 104 nm bathochromic shift was possible upon going from **2** to **8**, with the two azomethines differing only by a thiophene and one azomethine bond. Similarly, a 45 nm red shift was observed when increasing the number of azomethine bonds from two (**8**) to three (**9**). The trend was less pronounced when increasing the number of azomethine bonds from three to four (**10**), leading only to a 27 nm red shift. It is apparent that infinite absorbance shifts are not possible with multiple azomethine bonds. Nevertheless, color tuning covering 176 nm across the visible spectrum was readily possible by increasing the degree of conjugation. The collective spectra measured for the compounds in Figure 7 confirmed that simple structural modification, whether it be degree of conjugation or varying the number of thiophenes, greatly impacted the absorbance of the azomethines.

The fluorescence maximum of the azomethines was also sensitive to structural modifications. For example, the maxima shifted by 236 nm contingent on structure. The fluorescence of the azomethines in Figure 7 ranged between 480 and 716 nm. While their fluorescence could be measured, the fluorescence quantum yields (Φ_{fl}) were systematically low. In fact, the Φ_{fl} were $\leqslant 2\%$ when measured both against external references and using absolute methods including an integrating sphere at room temperature. This is not surprising since azomethines are known to undergo photoisomerization between their *E* and *Z* isomers [119–125]. However, photoisomers were not observed for any of the azomethine derivatives reported in this review.

The azomethine fluorescence could however be turned-on by protonating the amine [55]. Quantitative fluorescence revival was also observed at low temperature [126]. The collective fluorescence studies combined with the absence of triplet states observed by laser flash photolysis imply that the imine bond is responsible for quenching the singlet excited state. The deactivation modes were assigned to both intramolecular photoinduced electron transfer to the azomethine and possible rotation around the aryl-N bond [52]. The responsive fluorescence to environmental changes makes these conjugated azomethines interesting for sensor applications.

Similar to the optical properties, the electrochemical properties of the azomethines could significantly be modified contingent on structure. Of interest is the oxidation potential (E_{pa}). All the compounds had E_{pa} values above the reduction of oxygen, proving that they were air stable. While the effect of structural modification on the E_{pa} was less pronounced than what was observed for the spectroscopic properties, the E_{pa} could nonetheless be varied by 390 mV between 0.78 and 1.17 V (Figure 9). Most interesting was the reversibility of the oxidation process. Azomethines with hydrogens in the terminal positions underwent irreversible oxidation. Cursory interpretation of this result would suggest that the azomethines are oxidatively unstable and decompose. However, the electrochemically generated radical cation sustained anodic polymerization according to standard means to afford conjugated polymers [127]. In contrast, the oxidation process was reversible for the azomethines containing amines in the terminal positions, such as **8–10**. This confirmed that the resulting radical cation was stable and that the azomethines were oxidatively robust. Unlike the anodic process, the cathodic process generates the radical anion was irreversible. The origins of the irreversible cathodic process are unknown and they are currently being investigated.

4.3 Heterocyclic azomethines

Thiophene azomethine derivatives were originally examined owing to the known thermal and chemical stability of the thiophene moiety and its low oxidation potential. However, azomethines derived from other 5-membered aromatic heterocycles were also possible. Varying the π-richness/aromaticity with different heterocycles would impact the

azomethine opto-electronic properties in a similar way to that observed with structural modifications. It should therefore be possible to tune the colors by incorporating different heterocycles into the azomethines in addition to making symmetric and unsymmetric compounds. Azomethines incorporating furans, thiophenes, pyrroles, and 3,4-ethylenedioxithiophenes (EDOT) were prepared and examined. These heterocycles were selected because of their different aromaticity indices. For example, the aromaticity index of thiophene is 0.75, pyrrole is 0.59, furan is 0.46, while that of benzene is 1 [128]. A highly aromatic derivative would stabilize the azomethine, therefore decreasing its E_{pa}. Tuning the HOMO energy levels is therefore possible contingent on the different 5-membered heterocycles.

The different heterocyclic azomethines investigated are shown in Figure 10. From the collective spectroscopic data of the dyads and triads, it was found that the absorbance could be tailored as a function of the heterocycle. Because of their low aromaticity, the absorbance of the furan derivatives was blue shifted relative to the other heterocyclic azomethines. This was evidenced by the 15 nm hypsochromic shift between the homologues **16** and **4**. The pyrrole derivatives **19** and **21** were found to have the highest absorbance wavelengths of the heterocyclic azomethines investigated. This was owing to the strong π-donor character of the pyrrole compared to thiophene or furan. This resulted in a highly conjugated electronic *push-pull* system occurring between the pyrrole and the electron withdrawing ester groups of the central thiophene. This was confirmed by the 5 nm red shift observed for **21** relative to **19** as a result of strong electron donating character of *N*-methyl-pyrrole moiety.

Unsymmetric derivatives were also prepared to examine the effect of combining different heterocycles on the spectroscopic properties. For example, **15** had both a thiophene and *N*-methyl-pyrrole and exhibited the same absorbance as its all methyl-pyrrole analogue, **21**. Similarly, when substituting thiophene with furan, as in **14**, the absorbance was hypsochromically shifted by 20 nm in comparison to **4**. Finally, combining the strong π-donating *N*-methyl-pyrrole with the weakly aromatic furan, resulted in an electronic *push-pull* system (**23**) that was bathochromically shifted by 12 nm relative to the benchmark **4**. Absorbance tailoring covering 45 nm between 420 and 465 nm was therefore possible with unsymmetric azomethines by combining various 5-membered heterocycles.

While a wide range of absorbances were possible by incorporating different heterocycles, the effect was less pronounced on the E_{pa}. The azomethines all possessed E_{pa} that varied by only 200 mV, between 0.9 and 1.1 V. The electrochemical data confirmed that the azomethines were all stable under ambient conditions. The lowest E_{pa} measured was for **21**, whose E_{pa} was 200 mV less positive than the other azomethines. This was a result of the strong electron donating character of the pyrrole.

The reversibility of the anodic process was also contingent on substitution at the terminal positions of the heterocycles, similar to what was observed for the other compounds in Figure 7. The anodic process was irreversible with hydrogens substituted in the terminal positions such as **14–16**, **19**, and **23–25**. In contrast, the process was reversible with either methyl or amine substituents in the terminals position such as **17**, **18**, **20**, **22**, **26**. The electron donating character of the methyl groups located on the terminal positions additionally contributed to lowering the HOMO energy levels. As a result, the absorbance of the methylated derivatives was bathochromically shifted by ca. 40 nm relative to their hydrogen terminated analogues.

Given the strong absorbance of these azomethines in the

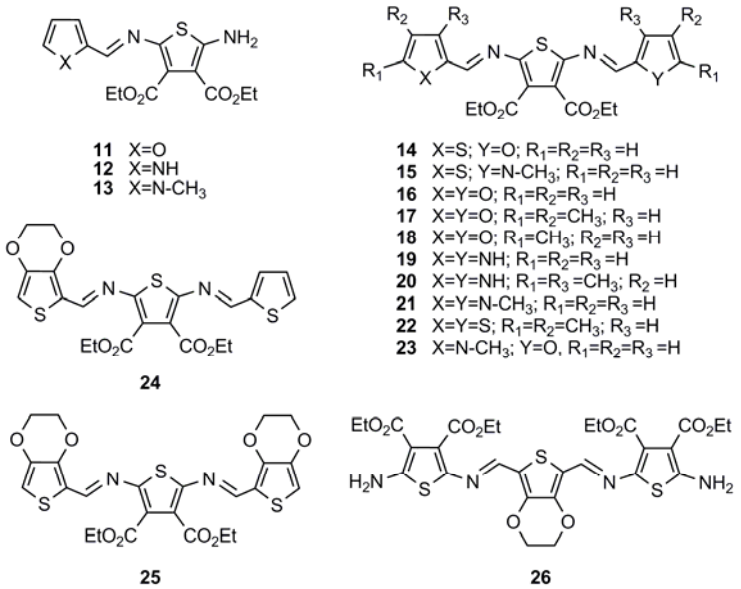

Figure 10 Various azomethines derived from different 5-membered heterocyclic aromatics.

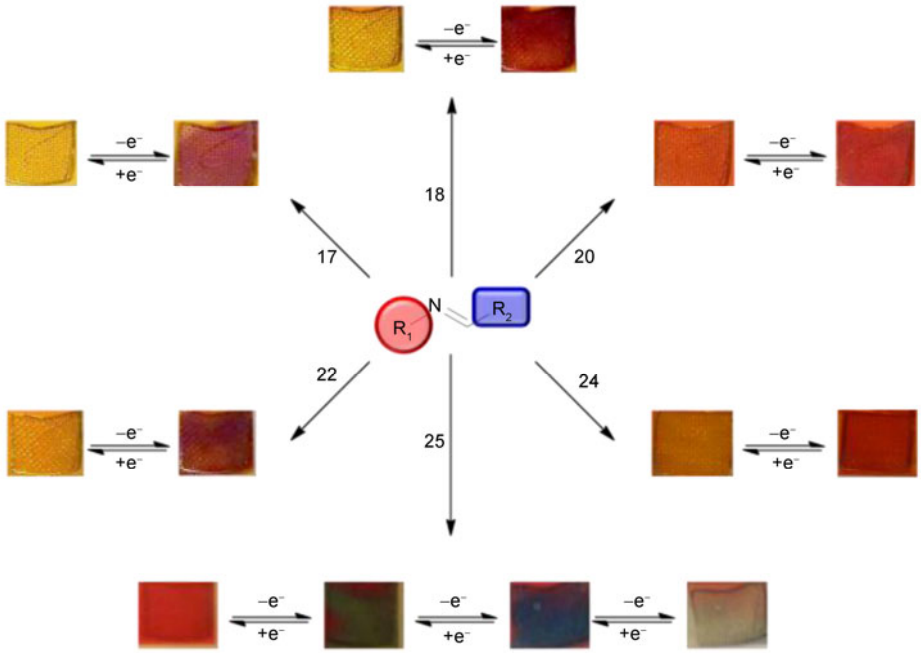

Figure 11 Colors of the neutral and oxidized states of the various thiophenoazomethines from Figure 10 observed on a platinum mesh electrode.

visible, their corresponding radical cations exhibited significantly different colors. This resulted in a high color contrast ratio between the neutral and oxidized states. For example, a 70 nm electrochemically induced change in the absorbance was observed for **22**. This resulted in a color change from orange to purple [129]. Both the color of the neutral and oxidized states were enhanced by incorporating the electron rich 3,4-ethylenedioxithiophene (EDOT) as was the case with **26** [130]. This was further an interesting derivative because it possessed three oxidation states. As a result, four discrete colors were observed when applying different potentials ranging between 0 and 2 V. The resulting reversible colors observed were red, green, blue, and transparent (Figure 11). The latter is a result of an absorbance occurring in the NIR at 950 nm and not from bleaching of the compound, which would indicate azomethine decomposition. Both the reversible oxidation and bold colors in the visible region of the spectrum make these azomethines viable candidates for electrochromic applications [131].

In addition to electrochemical oxidation, the azomethines could additionally be doped with both TFA and ferric chloride ($FeCl_3$) (Figure 12). Similar colors were observed when the azomethines were chemically and electrochemically doped (*vide infra*). In the case of the chemical dopants, the azomethines could be doped and undoped repeatedly without any spectroscopically (absorbance and NMR) detectable color degradation. This illustrates their robustness and resistance towards hydrolysis. Triethylamine was used as the dedopant when doping with TFA and hydrazine hydrate was similarly used as the dedopant when doping with ferric chloride.

Figure 12 Reversible color changes between neutral (top) and doped (bottom) states of **18**, **35**, **36**, and **37** (from left to right) when doped with either TFA or $FeCl_3$ in dichloromethane and neutralized with either triethylamine or hydrazine hydrate.

4.4 Electronic *push-pull* azomethines

Incorporating electron donating and withdrawing groups was also examined for tuning the azomethine opto-electronic properties (Figure 13). It was expected that incorporating various electronic groups in the terminal positions would dramatically perturb the HOMO energy levels to yield azomethines with bold colors spanning the visible spectrum. Furthermore, incorporating complementary electron withdrawing and donating groups in the terminal positions would result in an electronic *push-pull* system. This in turn would form an intramolecular charge transfer (ICT) complex, which is known to strongly absorb in the visible

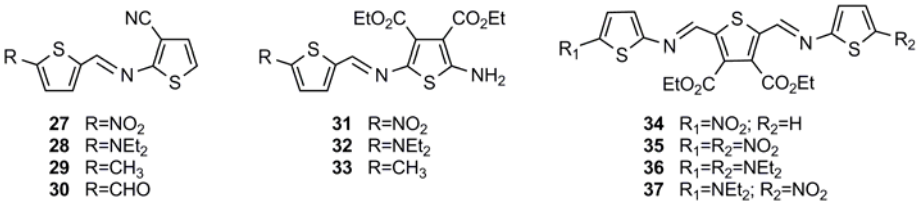

27 R=NO_2
28 R=NEt_2
29 R=CH_3
30 R=CHO

31 R=NO_2
32 R=NEt_2
33 R=CH_3

34 R_1=NO_2; R_2=H
35 R_1=R_2=NO_2
36 R_1=R_2=NEt_2
37 R_1=NEt_2; R_2=NO_2

Figure 13 Thiophenoazomethines incorporating strong electron donating and withdrawing groups in the terminal positions.

region [132].

The impact of the electron donating and withdrawing groups was surprisingly noticeable with the dyads. Interestingly, the *N*,*N*-diethylamine substituent caused the most significant change in the absorbance spectrum compared to its complementary electron withdrawing nitro group. This is evident by a 100 nm bathochromic shift observed for **28** relative to **1**, whereas the corresponding nitro derivative **27** was red shifted by only 30 nm. As expected for the weaker electron withdrawing aldehyde, the absorbance of **30** was red shifted by only 15 nm relative to **1**.

The effect of the electronic groups on the optical properties was similar for the trimers. For example, **34** and **35** both exhibited bathochromic shifts of 25 and 36 nm, respectively, compared to the unsubstituted homologue **4**. Meanwhile, **36** was red shifted by 110 nm relative to the benchmark azomethine **4**. The spectroscopic change was most pronounced for the complementary electronic *push-pull* azomethine **37** that was bathochromically shifted by 157 nm relative to **4**. The collective measured absorbance spectra are summarized in the top panel of Figure 14. It is evident that discrete absorbances spanning nearly 250 nm across the entire visible spectrum were possible by incorporating electron donating or withdrawing groups in the terminal positions of the dyad and triad azomethine derivatives. The color tuning of the compounds is further epitomized in the photographs in the middle panel of Figure 14. It is apparent that colors ranging between yellow and blue were possible via structural modification of the thiophenoazomethines. The colors can further be enhanced by chemical doping, as seen in the lower panel of Figure 14. For example, **8** changes from red to green, while **26** goes from red to blue, and **37** changes from blue to pink when doped with $FeCl_3$.

In addition to color tailoring, the E_{pa} could also be adjusted courtesy of the different electronic groups. Incorporating the electron donating amine lowered the E_{pa} by 300 mV relative to **1**. In contrast, the E_{pa} was increased by the presence of an electron withdrawing group. These effects were enhanced with the triads. For example, the highest E_{pa} were observed with **34** and **35**. The electronic *push-pull* **37** had a higher E_{pa} than **36**. The reduction potentials (E_{pc}) were also contingent on the electron donating or withdrawing groups. For example, the electron withdrawing group lowered the E_{pc}. Meanwhile, a reduction process was not observed for **36**. The collective electrochemical data demonstrated that the HOMO and LUMO energy levels, and in turn the energy gap, could be adjusted between 1 and 2.5 eV by incorporating various electronic groups into the terminal positions.

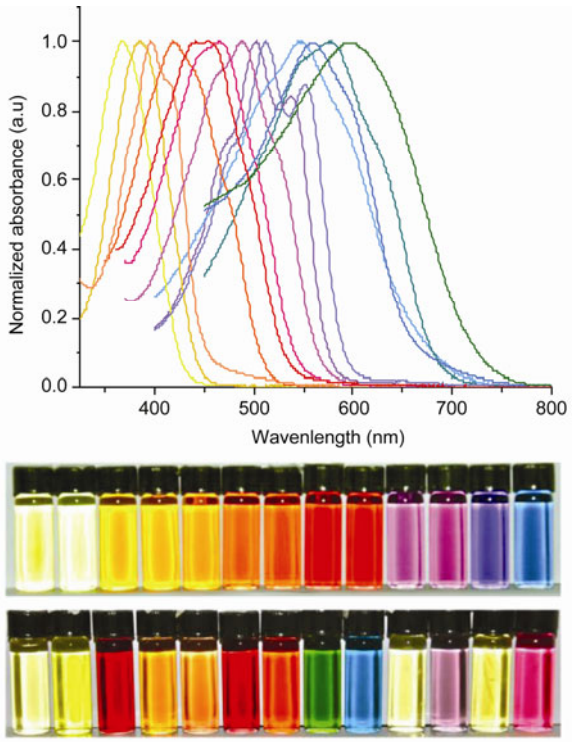

Figure 14 Top: normalized absorbance spectra of **11** (—), **13** (—), **18** (—), **14** (—), **4** (—), **22** (—), **35** (—), **8** (—), **26** (—), **9** (—), **36** (—), **10** (—), and **37** (—), measured in dichloromethane. Middle: solutions of **11** (—), **13** (—), **18** (—), **14** (—), **4** (—), **22** (—), **35** (—), **8** (—), **26** (—), **9** (—), **36** (—), **10** (—), and **37** (—) in dichloromethane. Bottom: solutions of **11** (—), **13** (—), **18** (—), **14** (—), **4** (—), **22** (—), **35** (—), **8** (—), **26** (—), **9** (—), **36** (—), **10** (—), and **37** (—) doped with $FeCl_3$.

4.5 Crystallographic studies

Useful structural information can be derived from single crystal X-ray diffraction (XRD) data of crystal structures. In the case of azomethines, XRD played an important role in assigning the absolute configuration of the azomethine bond. This was of importance because neither the *E* nor *Z* isomer could unequivocally be assigned by standard methods such as NMR. In all the cases of the thiophene containing azomethines that yielded suitable crystals for XRD, the *E* iso-

mer was consistently and exclusively observed. In some respects, this was not surprising since this is the most thermodynamically stable of the two isomers. What was of interest was that crystals of **4** and **8** did not photoisomerize to the *Z* isomer upon irradiation [133]. This was surprising since homoraryl azomethines have recently been found to undergo *E* to *Z* photoisomerization, even in the solid state [119, 134, 135]. The observed photostability is most likely a result of the high degree of conjugation of thiophenoazomethines.

XRD data provided additional useful structural information that could be correlated with the spectroscopic data. Of particular interest was the mean plane angle between the azomethine and the aryl-N planes. Small twisting angles would be observed with highly conjugated azomethines. In contrast larger twisting angles, resulting from steric hindrance between the *ortho* substituents on the N-aryl moiety and azomethine hydrogen, would limit the degree of conjugation. Such twisting was found for homoaryl azomethines (*vide supra*). However, there are few crystallographic accounts relating to thiophene containing azomethines. For this reason, we were motivated to examine the effect of different aryl groups connected to thiophenes via an azomethine. This was to provide important information relating to the twisting angle between the azomethine and aryl planes as a function of aryl derivatives. The crystallographic structures of the azomethines shown in Figure 15 were therefore resolved.

The XRD data of **38** confirmed that it had a similar mean plane angle to its all benzene analogues in Figure 5 [67]. The thiophene-azomethine mean plane was twisted by 86° from the benzene mean plane, which is evidenced in Figure 16(a) [52]. This was in contrast to a twisting angle of only 44° for the analogue of **38** having hydrogens in the *ortho* positions [52]. The large twist angle from coplanarity was a result of the steric hindrance between the bulkyl *tert*-butyl groups in the *ortho* position and the azomethine hydrogen. The large twist angle suggested that the rotational barrier around aryl-N was extremely high. This was confirmed using theoretical calculations for **38**, which was used a model compound to investigate the origins of the quenched fluorescence of thiophene containing azomethines [136]. The collective XRD data, rotational barrier calculations and quenching studies of **38** confirmed that the quenched fluorescence of thiophene azomethines involved rotational deactivation and intramolecular photoinduced electron transfer [52, 54, 136–138].

The XRD data of **38** confirmed that azomethines derived from 2-thiophene carboxaldehyde and 6-membered homoarylamines did not afford highly coplanar azomethines. This was further supported by the XRD data of both **39** and **40**. The twisting angle between the quinoline and the thiophene mean planes of **39** was 37.27 (5)° [139]. The observed deviation from coplanarity was once again a result of steric hindrance between the azomethine hydrogen and the hydrogen in the 4-position of the quinoline.

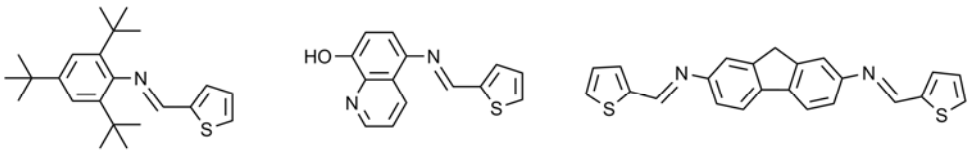

38 **39** **40**

Figure 15 Homocyclic azomethines coupled with thiophene investigated by XRD.

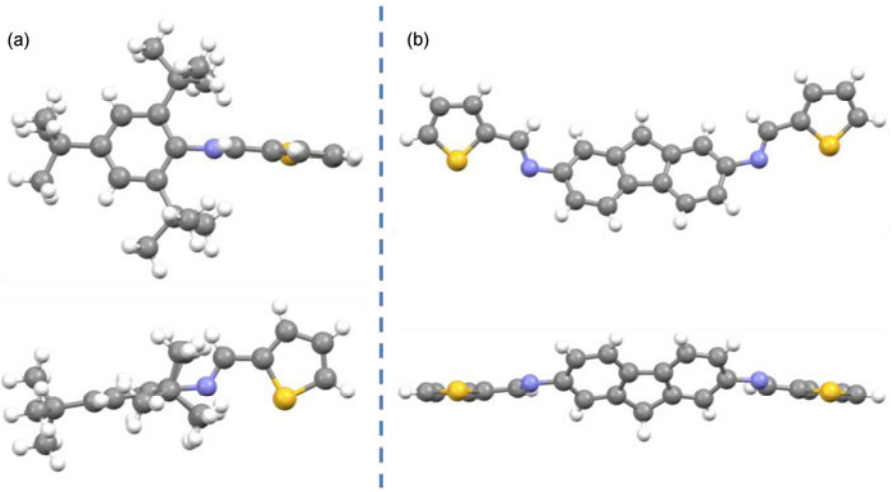

Figure 16 (a) Face (top) and edge (bottom) view of the crystal structure of **38** showing the twisting between the benzene and azomethine planes; (b) face (top) and edge (bottom) view of the crystal structure of **40** illustrating the twisting between the fluorene and azomethine planes.

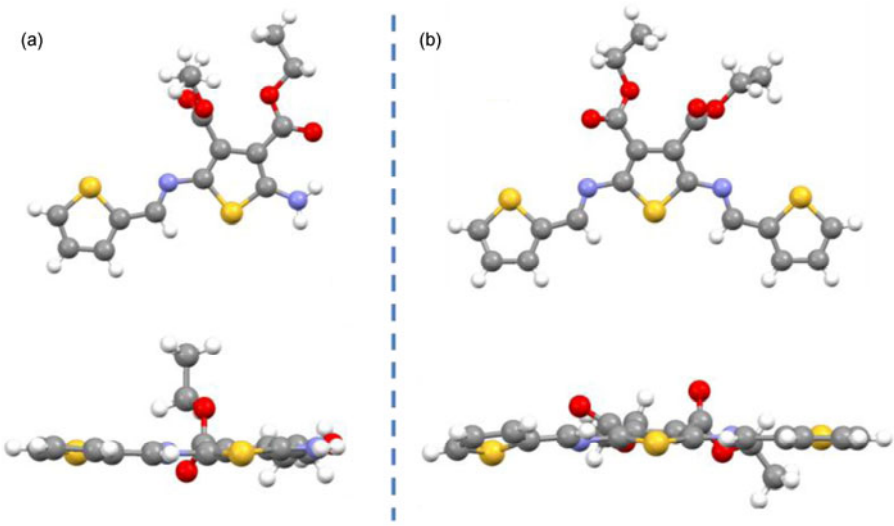

Figure 17 (a) Face (top) and edge (bottom) view of the crystal structure of **2**; (b) face (top) and edge (bottom) view of the crystal structure of **4**.

Fluorene incorporation did not further reduce the twisting between the aryl and azomethine mean planes. The measured mean plane angles between the central fluorene and its terminal azomethines of **40** were 48.06 (7)° and 45.85 (7)° [54]. The twisting of the mean planes for minimizing the steric hindrance between the azomethine hydrogen and those in the fluorene 2- and 9-positions is evident in Figure 16(b).

Suitable crystals for XRD analysis were obtained for many of the thiophene derivatives from Figures 7, 10, and 13. The striking difference between the structures resolved for the azomethines in these figures and those of **38–40** was the Smaller torsion angle between the thiophene and azomethine planes. A larger bite angle (126°) between the *ortho* substituent and the azomethine bond was observed for the all-heterocyclic derivatives relative to their 6-membered aryl counterparts (120°). In the case of the thiophenoazomethines, the adjacent thiophenes adopted an *anti*-configuration. While this arrangement placed the *ortho*-ester of **DAT** and the azomethine hydrogen in the same plane, they are *anti*-parallel and they are not within contact distance, as seen in Figure 17. The differences between the all-thiophene and benzyl azomethine derivatives were further evidenced when comparing the crystal structures of **2** and **4** (Figure 4). The *anti*-configuration also encourages favorable intramolecular hydrogen bonding between the **DAT** sulfur and the azomethine hydrogen. The net effect is the absence of steric hindrance between the *ortho* substituents and the azomethine hydrogen, resulting in much higher coplanarity between the thiophenes and azomethines to which they are connected [140, 141]. For example, the torsion between the thiophene and azomethine mean planes was 7.25 (11)° for **2** [140]. Similarly, reduced mean plane torsion angles were also observed for **4** and **6**. In the case of **4**, the planes of the terminal thiophenes were twisted by 9.04 (4)° and 25.07 (6)° from the CH=N–thiophene–N=CH plane [133, 141]. Interestingly, the corresponding mean plane torsion angles for **6** were smaller, being 2.6° and 8.0° [118]. In fact, the corresponding mean plane angle for the azomethines in Figures 7, 10, and 13 varied between 1.9° and 27° [142–148]. In general, substituents larger than hydrogens can be incorporated into the *ortho* position with minimal effect to the thiophene-azomethine torsion angle. Moreover, the reduced mean plane torsion angle of the thiophenoazomethines is in part responsible for their increased degree of conjugation relative to their homoaryl counterparts.

The XRD data for the all-thiophene azomethines suggests that 5-membered heterocyclic azomethines should all have small torsions between the aryl and azomethine planes. However, exceptions were observed, especially with certain pyrrole and furan azomethine derivatives. In the case of the pyrrole azomethine derivatives, the mean plane angle between the pyrrole and azomethine planes was larger than that of the corresponding all-thiophene counterpart. For example, the mean plane angle between the methyl-pyrrole and azomethine-thiophene-azomethine planes for **12** was 17.06 (4)° [143]. The larger torsion angle was most likely a result of increased steric hindrance between the methyl-pyrrole and the azomethine hydrogen, which was suggested by the increased pyrrole disordered observed in the XRD. As opposed to the all-thiophene azomethine derivatives that exclusively adopted the *anti*-conformer, the pyrrole-thiophene adopted a mixture of both the *anti*- and *syn* conforms. A 73:27 ratio was found between the *syn* and *anti* conformers, with respect to the pyrrole-thiophene orientation. Interestingly, the pyrroles of **21** were highly ordered. However, it had mean plane torsion angles that were 14.44 (4)° and 27.30 (7)° [129]. The twisting of the pyrrole from the azomethine plane was also found even with the N–H pyrrole **19**. The dihedral angles between the pyrroles and the thiophene were 10.31 (4)° and 18.90 (5)° [142]. In contrast, the heterocycles and the azomethines of the unsym-

metric **15** were coplanar, with mean plane torsion angles of 2.3 (2)° and 2.5 (3)° [145].

Torsional angles between the heterocyclic and azomethine planes for the furan derivatives were also consistently smaller than their 6-membered homoaryl counterparts. The mean plane for the furan in **11** was twisted by only 2.51 (4)° from the azomethine-thiophene mean plane [144]. This was in contrast to **16** whose furan mean plane angles were twisted by 7.33 (4)° and 21.74 (5)° from the azomethine mean plane [146]. Different torsional angles for the two terminal heterocycles were similarly observed with **4**. This was in contrast to **23** where the mean plane angles of both the furan and *N*-methyl pyrrole with respect to the azomethine-thiophene mean plane were essentially identical; 18.0 (2)° and 18.8 (2)° [126]. The smallest torsion angle was observed with the EDOT derivative **25**, whose deviation from coplanarity was only 1.9 (3)° [147].

The crystal lattice organization for the all-thiophene azomethines was similar. They were all highly crystalline owing to many intra- and intermolecular interactions. For example, both **4** and **6** had intramolecular hydrogen bonding between the sulfur of the central thiophene and the azomethine hydrogen (*vide supra*). Despite their similarities, they differed in their packing arrangement. **4** adopted a ladder-type configuration that resulted from intermolecular hydrogen bonding between the hydrogen in the 3-position of the external thiophene and the ester oxygen. π-Stacking also occurred between the thiophenes and the azomethine in addition to C–H–π interactions. These led to a densely packed network with each thiophenoazomethine packed in an *anti*-parallel arrangement [133]. Similarly, hydrogen bonding was also found for **6**. However, these interactions took place between the ester hydrogen and the ester oxygen of different molecules. Hydrogen bonding between the ester oxygen and the azomethine hydrogen were also found. In contrast to **4**, π-stacking was observed between the bithiophenes for **6** (Figure 18) [118].

The observed packing differences in the solid state were a result of subtle structural modifications that led to different intra- and intermolecular interactions. For example, the *N*-methylpyrrole derivatives **12** and **21** were found to have π-stacking between the intercalated thiophenes in addition to hydrogen bonding between the terminal amine and the ester hydrogen for **12** and the esters for **21**. These led to a

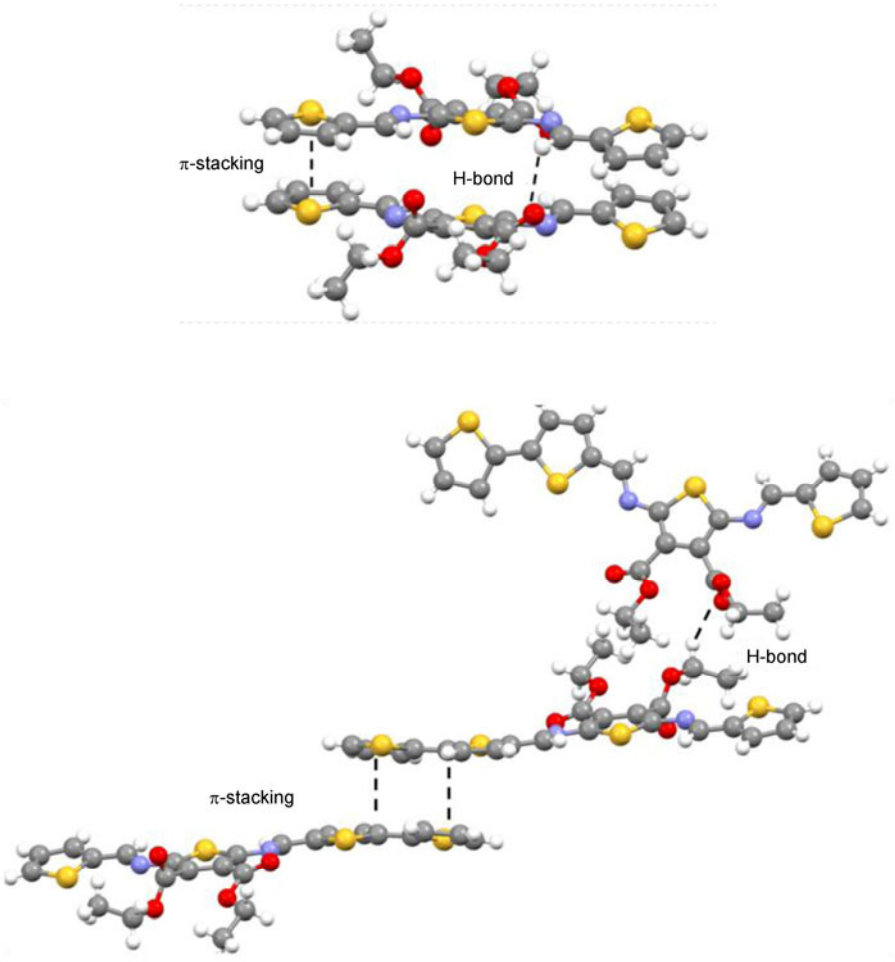

Figure 18 Crystal lattice packing of **4** (top) and **6** (bottom).

herringbone packing structure. This is in contrast to the N–H pyrrole derivative **19** where π-stacking was not observed in its herringbone type crystal packing. The strong N–H hydrogen donor site of the pyrrole was a driving force for the crystallization of **19** via N–H···O and N–H···N donor-acceptor interactions. C–H···N and C–H···O interactions were also observed. Meanwhile, the unsymmetric **15** showed no hydrogen-bonding and only π-stacking in the crystal lattice. Additional intermolecular interactions were also observed with the various heterocyclic azomethines including sulfur-hydrogen, hydrogen bonding, and heteroatom-aryl intermolecular interactions involving the heteroatoms of the different heterocycles. The collective XRD data confirmed that the exact crystal packing cannot be predicted owing to intra- and intermolecular interactions that are specific to each heterocycle. Nevertheless, these interactions play important roles, not only in making the azomethines crystalline, but also for their high degree of conjugation and their enhanced optical properties relative to their all-carbon counterparts.

The C=N bond length was another interesting property that could accurately be assessed from the XRD data. This was of importance given that the CH=N and CH=CH bonds are assumed to be isoelectronic. The XRD data of the heterocyclic azomethines was consistently found to be ca. 1.27 Å. Within experimental error, the length of the azomethine bond was marginally shorter than its vinylene counterpart, whose CH=CH bond length was 1.3 Å [149].

4.6 Thiophene Polyazomethines

In pursuing the use of mild conditions for preparing conjugated azomethines, we applied the method used for the preparation of small molecule azomethines to prepare polymers. The objective was to prepare the polymer **41** (Figure 19) and its derivatives consisting uniquely of thiophenes. Motivation for the preparation of **41** and its derivatives was due in part to the fact that such polymers had not previously been reported, especially those derived from **DAT**. Similar to the thiophene dyad and triad azomethines, enhanced optical and electrochemical properties were expected with **41** relative to polyazomethines derived from phenylene diamine. The additional advantage expected of **41** was its limited intermolecular π-stacking. This would make it more soluble in common organic solvents compared to its homoaryl counterparts that have limited solubility in *N,N*-dimethylacetamide and *N,N*-dimethylformamide [65, 150–152]. The C10 alkylated thiophene dialdehyde was used as the comonomer with **DAT** to ensure that **41** was soluble in common solvents, allowing it to be subsequently characterized. Of particular interest was measuring the polymer molecular weight by standard techniques, which was challenging with homoraryl polyazomethines.

The targeted **41** was successfully polymerized under reduced pressure in refluxing chloroform with a catalytic amount of TFA [153]. This was in contrast to previously reported methods of homoaryl azomethine poylmerization that required $TiCl_4$, organic bases, polar solvents, and high boiling temperatures [154]. The advantages of the mild polymerization of **41** was that the resulting polymer would be used *as-is*. It did not require purification since there are no by-products. Alternatively, it could be precipitated in methanol to remove lower molecular weight oligomers and then redissolved in common organic solvents including THF, dichloromethane, acetonitrile, and chloroform. The added advantage of **41** being soluble in both THF and chloroform is that its molecular weight could be measured both by GPC and NMR. Both characterization methods were consistent and they confirmed that **41** was a polymer having M_n of 15 kg/mol and a PDI of 1.3 [155]. The polymerization of **41** was found to follow standard step-growth polymerization and not undergo dynamic component exchange. The latter is typical for imine containing polymers [156–160].

The electrochemical properties of **41** were interesting such that it could be oxidized and reduced. This makes it an interesting p- and n-type material. The measured energy gap from electrochemistry was 1.5 eV, but it had a sufficiently high E_{pa} to be air stable. Its LUMO energy level (–3.8 eV) was found to be compatible with the standard acceptor material used in organic photovoltaics, $PC_{60}BM$. Similarly, the HOMO energy level (–4.8 eV) of **41** was compatible with the commonly used ITO anode. The collective electrochemical properties, taken together with the broad absorbance in the visible region ranging between 400 and 800 nm, make **41** an interesting photoactive layer for photovoltaic applications. Meanwhile, its strong absorbance in the visible range and its reversible oxidation were exploited for electrochromic applications [161].

Step-growth polymers possess complementary termini that can undergo polymerization reactions. While this was demonstrated with other step-growth polymers [162–164], it had not been reported for polyazomethines. It was found

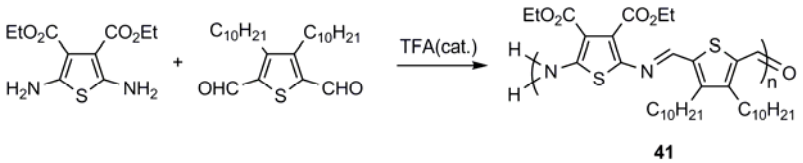

41

Figure 19 Polymerization scheme of **41**.

that the molecular weight of **41** could be increased. This was possible by taking pristine **41**, isolated by precipitation, and dissolving the resulting powder in THF. Molecular weight increase was possible through repolymerization of **41** by heating it with a catalyst.

The reactivity of the terminal aldehyde of **41** was also exploited for postpolymerization functionalization. The terminal aldehyde underwent reductive amination with a yellow amino-dansyl dye to change the original color of the polymer from blue to green. The molecular weight of the polymers could also be increased via reductive amination of the terminal aldehyde with α,ω-dodecyl diamine. The robustness of the conjugated azomethines along the polymer backbone was epitomized by its resistance towards reduction during the selective reductive amination reaction involving the terminal aldehyde [165].

5 Summary and future prospects

The highly π-conjugated azomethines consisting entirely of 5-membered heterocycles serve to illustrate that robust materials having properties suitable for opto-electronic applications are possible. The properties can be readily tailored via simple structural changes such as the number of azomethines, type of aryl heterocycle, and by incorporating various electronic groups. With colors spanning 250 nm across the visible spectrum and reversible oxidation, azomethines are ideal candidates for electrochromic applications. Meanwhile, the ease of azomethine preparation and minimal purification make them suitable alternate replacements for vinylene counterparts, especially in light of their oxidative, hydrolytic, and reductive robustness. The broad range of properties that can be tuned by straightforward structural modification makes azomethines interesting as universal functional materials. The azomethine property tuning is further interesting in that the opto-electronic properties can be tailored to meet the performance requirements for a wide gamut of applications and devices.

Financial support for the original publications was provided by NSERC Canada in the form of a Discovery Grant, Strategic Research Grants, Idea-to-Innovation, and Research Tools and Instruments grants in addition to CFI for additional equipment funding. WGS also thanks both the Alexander von Humboldt Foundation and the RSC for a JWT Jones Travelling fellowship, allowing the completion of this manuscript. AB acknowledges both NSERC and the Université de Montréal for graduate scholarships. The authors also thank the numerous highly qualified personnel that made significant contributions to the thiophenoazomethine projects during the recent years.

1 Chiang CK, Fincher CRJ, Park YW, Heeger AJ, Shirakawa H, Louis EJ, Gau SC, MacDiarmid AG. Electrical conductivity in doped polyacetylene. *Phys Rev Lett*, 1977, 39(17): 1098–1101

2 Morin JF, Leclerc M, Adès D, Siove A. Polycarbazoles: 25 years of progress. *Macromol Rapid Commun,* 2005, 26(10): 761–778

3 Klärner G, Müller M, Morgenroth F, Wehmeier M, Soczka-Guth T, Müllen K. Conjugated oligomers and polymers —New routes, new structures. *Synthetic Met*, 1997, 84(1-3): 297–301

4 Rasmussen SC, Schwiderski RL, Mulholland ME. Thieno[3,4-b]pyrazines and their applications to low band gap organic materials. *Chem Commun,* 2011, 47(41): 11394–11410

5 Mishra A, Ma CQ, Bäuerle P. Functional oligothiophenes: Molecular design for multidimensional nanoarchitectures and their applications. *Chem Rev*, 2009, 109(3): 1141–1276

6 Schlüter AD. The tenth anniversary of suzuki polycondensation (spc). *J Polym Sci Pol Chem*, 2001, 39(10): 1533–1556

7 Chemli M, Haj Said A, Fave JL, Barthou C, Majdoub M. Synthesis and chemical modification of new luminescent substituted poly(p-phenylene) polymers. *J Appl Polym Sci,* 2012, 125(5): 3913–3919

8 Senkovskyy V, Tkachov R, Beryozkina T, Komber H, Oertel U, Horecha M, Bocharova V, Stamm M, Gevorgyan SA, Krebs FC, Kiriy A. "Hairy" poly(3-hexylthiophene) particles prepared via surface-initiated kumada catalyst-transfer polycondensation. *J Am Chem Soc*, 2009, 131(45): 16445–16453

9 Tam TL, Tan HHR, Ye W, Mhaisalkar SG, Grimsdale AC. One-pot synthesis of 4,8-dibromobenzo[1,2-d;4,5-d']bistriazole and synthesis of its derivatives as new units for conjugated materials. *Org Lett*, 2011, 14(2): 532–535

10 Van den Bergh K, De Winter J, Gerbaux P, Verbiest T, Koeckelberghs G. Ni-catalyzed polymerization of poly(3-alkoxythiophene)s. *Macromol Chem Phys*, 2011, 212(4): 328–335

11 Pei J, Wen S, Zhou Y, Dong Q, Liu Z, Zhang J, Tian W. A low band gap donor-acceptor copolymer containing fluorene and benzothiadiazole units: Synthesis and photovoltaic properties. *New J Chem*, 2011, 35(2): 385–393

12 Cheng YJ, Luh TY. Synthesizing optoelectronic heteroaromatic conjugated polymers by cross-coupling reactions. *J Organomet Chem*, 2004, 689(24): 4137–4148

13 Berrouard P, Najari A, Pron A, Gendron D, Morin P-O, Pouliot J-R, Veilleux J, Leclerc M. Synthesis of 5-alkyl[3,4-c]thienopyrrole-4,6-dione-based polymers by direct heteroarylation. *Angew Chem Int Ed*, 2012, 51(9): 2068–2071

14 Hofmann S, Thomschke M, Lüssem B, Leo K. Top-emitting organic light-emitting diodes. *Opt Express*, 2011, 19(S6): A1250–A1264

15 Chen S, Deng L, Xie J, Peng L, Xie L, Fan Q, Huang W. Recent developments in top-emitting organic light-emitting diodes. *Adv Mater*, 2010, 22(46): 5227–5239

16 Zhong C, Duan C, Huang F, Wu H, Cao Y. Materials and devices toward fully solution processable organic light-emitting diodes. *Chem Mater*, 2010, 23(3): 326–340

17 Zhang F, Wu D, Xu Y, Feng X. Thiophene-based conjugated oligomers for organic solar cells. *J Mater Chem,* 2011, 21(44): 17590–17600

18 Xue J. Perspectives on organic photovoltaics. *Polymer Rev*, 2010, 50(4): 411–419

19 Beaujuge PM, Reynolds JR. Color control in π-conjugated organic polymers for use in electrochromic devices. *Chem Rev*, 2010, 110(1): 268–320

20 Mortimer RJ, Dyer AL, Reynolds JR. Electrochromic organic and polymeric materials for display applications. *Displays*, 2006, 27(1): 2–18

21 Haubner K, Jaehne E, Adler HJP, Koehler D, Loppacher C, Eng LM, Grenzer J, Herasimovich A, Scheiner S. Assembly, structure, and performance of an ultra-thin film organic field-effect transistor (OFET) based on substituted oligothiophenes. *Org Electron*, 2009, 75–94

22 Yumusak C, Sariciftci NS. Organic electrochemical light emitting field effect transistors. *Appl Phys Lett*, 2010, 97(3): 033302

23 Aleshin AN, Shcherbakov IP, Petrov VN, Titkov AN. Solution-processed polyfluorene-zno nanoparticles ambipolar light-emitting field-effect transistor. *Org Electron*, 2011, 12(8): 1285–1292

24 Okamoto K, Luscombe CK. Controlled polymerizations for the synthesis of semiconducting conjugated polymers. *Polym Chem*, 2011, 2(11): 2424–2434

25 Starčević K, Boykin DW, Karminski-Zamola G. New amidino-benzimidazolyl thiophenes: Synthesis and photochemical synthesis. *Heteroat Chem*, 2003, 14(3): 218–222

26 Younes AH, Zhang L, Clark RJ, Davidson MW, Zhu L. Electronic structural dependence of the photophysical properties of fluorescent heteroditopic ligands-implications in designing molecular fluorescent indicators. *Org Biomol Chem,* 2010, 8(23): 5431–5441

27 Karacsony O, Deschamps JR, Trammell SA, Nita R, Knight DA. Synthesis of a 2,2'-bipyridyl functionalized oligovinylene-phenylene using heck and horner-wadsworth-emmons reactions and X-ray crystal structure of e-(4-(4-bromostyryl)phenyl)(methyl)sulfane. *Molecules*, 2012, 17: 5724–5732

28 Patil PS, Haram NS, Pal RR, Periasamy N, Wadgaonkar PP, Salunkhe MM. Synthesis, spectroscopy, and electrochemical investigation of new conjugated polymers containing thiophene and 1,3,4-thiadiazole in the main chain. *J Appl Polym Sci*, 2012, 125(3): 1882–1889

29 Jenekhe SA, Yang CJ, Vanherzeele H, Meth JS. Cubic nonlinear optics of polymer thin films. Effects of structure and dispersion on the nonlinear optical properties of aromatic schiff base polymers. *Chem Mater*, 1991, 3(6): 985–987

30 Schab-Balcerzak E, Grucela-Zajac M, Krompiec M, Niestroj A, Janeczek H. New low band gap compounds comprised of naphthalene diimide and imine units. *Synth Met*, 2012, 162(5–6): 543–553

31 Bolduc A, Dufresne S, Skene WG. Chemical doping of edot azomethine derivatives: Insight into the oxidative and hydrolytic stability. *J Mater Chem*, 2012, 22(11): 5053–5064

32 Jursic BS. Suitability of furan, pyrrole and thiophene as dienes for diels-alder reactions viewed through their stability and reaction barriers for reactions with acetylene, ethylene and cyclopropene. An am1 semiempirical and b3lyp hybrid density functional theory study. *Theochem*, 1998, 454(2-3): 105–116

33 Bourgeaux M, Skene WG. Photophysics and electrochemistry of conjugated oligothiophenes prepared by using azomethine connections. *J Org Chem*, 2007, 72(23): 8882–8892

34 Yang CJ, Jenekhe SA. Conjugated aromatic poly(azomethines). 1. Characterization of structure, electronic spectra, and processing of thin films from soluble complexes. *Chem Mater*, 1991, 3(5): 878–887

35 da Silva CM, da Silva DL, Martins CVB, de Resende MA, Dias ES, Magalhães TFF, Rodrigues LP, Sabino AA, Alves RB, de Fátima Â. Synthesis of aryl aldimines and their activity against fungi of clinical interest. *Chem Biol Drug Des*, 2011, 78(5): 810–815

36 Matharu BK, Sharma JR, Manrao MR. Aldimines: Synthesis and effect of molecule dimension on antifungal potential. *J Indian Counc Chem*, 2006, 23: 47–50

37 Rani N, Sharma JR, Manrao MR. Synthesis and comparative fungitoxicity of benzalbenzylamines and benzalanilines. *Pestic Res J*, 2006, 18: 129–132

38 Niazi S, Javali C, Paramesh M, Shivaraja S. Study of influence of linkers and substitutions on antimicrobial activity of some schiff bases. *Int J Pharm Pharm Sci*, 2010, 2: 108–112

39 Hania MM. Synthesis of some imines and investigation of their biological activity. *E-J Chem*, 2009, 6: 629–632

40 Ozkay Y, Incesu Z, Isikdag I, Yesilkaya M. Antiproliferative effects of some n-benzylideneanilines. *Cell Biochem Funct*, 2008, 26: 102–106

41 Han SY, Inoue H, Terada T, Kamoda S, Saburi Y, Sekimata K, Saito T, Kobayashi M, Shinozaki K, Yoshida S, Asami T. N-benzylideneaniline and *N*-benzylaniline are potent inhibitors of lignostilbene-α,β-dioxygenase, a key enzyme in oxidative cleavage of the central double bond of lignostilbene. *J Enzyme Inhib Med Chem*, 2003, 18: 279–283

42 Dronia H, Gruss U, Gaegele G, Friedrich T, Weiss H. Structure-activity analysis of fluorinated 1-n-arylamino-1-arylmethane-phosphonic acid esters as inhibitors of the nadh:Ubiquinone oxidoreductase (complex i). *J Comput-Aided Mol Des*, 1996, 10: 100–106

43 Pasayat S, Dash SP, Saswati, Majhi PK, Patil YP, Nethaji M, Dash HR, Das S, Dinda R. Mixed-ligand aroylhydrazone complexes of molybdenum: Synthesis, structure and biological activity. *Polyhedron*, 2012, 38(1): 198–204

44 Patel RN, Singh A, Shukla KK, Sondhiya VP, Patel DK, Singh Y, Pandey R. Design, synthesis, and characterization of a series of biologically active copper(II) schiff-base coordination compounds. *J Coord Chem*, 2012, 65: 1381–1397

45 Kerneghan PA, Halperin SD, Bryce DL, Maly KE. Postsynthetic modification of an imine-based microporous organic network. *Can J Chem*, 2011, 89(5): 577–582, S577/571-S577/516

46 Uribe-Romo FJ, Doonan CJ, Furukawa H, Oisaki K, Yaghi OM. Crystalline covalent organic frameworks with hydrazone linkages. *J Am Chem Soc*, 2011, 133(30): 11478–11481

47 Pandey P, Katsoulidis AP, Eryazici I, Wu Y, Kanatzidis MG, Nguyen ST. Imine-linked microporous polymer organic frameworks. *Chem Mater*, 2010, 22(17): 4974–4979

48 Uribe-Romo FJ, Hunt JR, Furukawa H, Klöck C, O'Keeffe M, Yaghi OM. A crystalline imine-linked 3-d porous covalent organic framework. *J Am Chem Soc*, 2009, 131(13): 4570–4571

49 Pattakaran RLR, Burkanudeen AR. Synthesis and characterization of epoxy-containing schiff-base and phenylthiourea groupes for improved thermal conductivity. *Polym-Plast Technol*, 2012, 51: 140–145

50 Zhang XH, Huang LH, Chen S, Qi GR. Improvement of thermal properties and flame retardancy of epoxy-amine thermosets by introducing bisphenol containing azomethine moiety. *Express Polym Lett*, 2007, 1(5): 326–332

51 Ayesha Kausar SZ, Ahmad Z, Muhammad IS. Novel processable and heat resistant poly(phenylthiourea azomethine imide)s: Synthesis and characterization. *Polym Degrad Stab*, 2010, 95: 1826–1833

52 Bourque AN, Dufresne S, Skene WG. Thiophene-phenyl azomethines with varying rotational barriers-model compounds for examining imine fluorescence deactivation. *J Phys Chem C*, 2009, 113(45): 19677–19685

53 Dong Y, Bolduc A, McGregor N, Skene WG. Push-pull aminobithiophenes-highly fluorescent stable fluorophores. *Org Lett*, 2011, 13(7): 1844–1847

54 Dufresne S, Perez Guarin SA, Bolduc A, Bourque AN, Skene WG. Conjugated fluorene-thiophenes prepared from azomethine connections part i. The effect of electronic and aryl groups on the spectroscopic and electrochemical properties. *Photochem Photobiol Sci*, 2009, 8(6): 796–804

55 Knipping É, Roche IU, Dufresne S, McGregor N, Skene WG. Selective fluorescence turn-on of a prefluorescent azomethine with Zn^{2+}. *Tetrahedron Lett*, 2011, 52(34): 4385–4387

56 Farcas A, Jarroux N, Ghosh I, Guégan P, Nau WM, Harabagiu V. Polyrotaxanes of pyrene-triazole conjugated azomethine and α-cyclodextrin with high fluorescence properties. *Macromol Chem Phys,* 2009, 210(17): 1440–1449

57 Sibel Derinkuyu KE, Oter O, Ergun Y. Ph-driver fluorescent switch behavior of azomethine dyes in solid matrix materials. *Spectrosc Lett*, 2010, 43: 500–512

58 Liu JL, Xu S, Yan B. Photoactive hybrids with the functionalized schiff-base derivatives covalently bonded inorganic silica network: Sol-gel synthesis, characterization and photoluminescence. *Colloids Surf A*, 2011, 373(1-3): 116–123

59 Sek D, Grabiec E, Janeczek H, Jarzabek B, Kaczmarczyk B, Domanski M, Iwan A. Structure-properties relationship of linear and star-shaped imines with triphenylamine moieties as hole-transporting materials. *Opt Mater,* 2010, 32(11): 1514–1525

60 Yen HJ, Liou GS. Novel blue and red electrochromic poly(azomethine ether)s based on electroactive triphenylamine moieties. *Org Electron*, 2010, 11(2): 299–310

61 Is OD, Koyuncu FB, Koyuncu S, Ozdemir E. A new imine coupled pyrrole-carbazole-pyrrole polymer: Electro-optical properties and electrochromism. *Polymer*, 2010, 51(8): 1663–1669

62 Gao Z, Yu Y, Xu Y, Li S. Synthesis and characterization of a liquid crystalline epoxy containing azomethine mesogen for modification of epoxy resin. *J Appl PolymSci*, 2007, 105(4): 1861–1868

63 Mallikharjuna Rao Darla SV. Synthesis and characterisation of azomethine class thermotropic liquid crystals and their application in non-linear optics. *Liq Cryst,* 2012, 39(1): 63–70

64 Iwan A, Bilski P, Janeczek H, Jarzabek B, Domanski M, Rannou P, Sikora A, Pociecha D, Kaczmarczyk B. Thermal, optical, electrical and structural study of new symmetrical azomethine based on poly(1,4-butanediol)bis(4-aminobenzoate). *J Mol Struct*, 2010, 963(2-3): 175–182

65 Iwan A, Palewicz M, Sikora A, Chmielowiec J, Hreniak A, Pasciak G, Bilski P. Aliphatic-aromatic poly(azomethine)s with ester groups as thermotropic materials for opto(electronic) applications. *Synth Met*, 2010, 160(17-18): 1856–1867

66 Hindson JC, Ulgut B, Friend RH, Greenham NC, Norder B, Kotlewski A, Dingemans TJ. All-aromatic liquid crystal triphenylamine-based poly(azomethine)s as hole transport materials for opto-electronic applications. *J Mater Chem*, 2010, 20(5): 937–944

67 Bürgi HB, Dunitz JD. Crystal and molecular structures of benzylideneaniline, benzylideneaniline-p-carboxylic acid and p-methylbenzylidene-p-nitroaniline. *Helv Chim Acta*, 1970, 53(7): 1747–1764

68 Hoekstra A, Meertens P, Vos A. Refinement of the crystal structure of trans-stilbene (TSB). The molecular structure in the crystalline and gaseous phases. *Acta Crystallogr, Sect B: Struct Sci*, 1975, 31(12): 2813–2817

69 Bartholomew GP, Bu X, Bazan GC. Preferential cocrystallization among distyrylbenzene derivatives. *Chem Mater*, 2000, 12: 2311–2318

70 Zhu S, Zhu S, Jin G, Li Z. Strong phenyl-perfluorophenyl π-π stacking and C–H···F–C hydrogen bonding interactions in the crystals of the corresponding aromatic aldimines. *Tetrahedron Lett*, 2005, 46(15): 2713–2716

71 Mallet C, Allain M, Leriche P, Frere P. Competition between π-π or furan-perfluorophenyl stacking interactions in conjugated compounds prepared from azomethine connections. *CrystEngComm*, 2011, 13(19): 5833–5840

72 Roncali J. Conjugated poly(thiophenes): Synthesis, functionalization, and applications. *Chem Rev*, 1992, 92(4): 711–738

73 McCullough RD, Tristram-Nagle S, Williams SP, Lowe RD, Jayaraman M. Self-orienting head-to-tail poly(3-alkylthiophenes): New insights on structure-property relationships in conducting polymers. *J Am Chem Soc*, 1993, 115(11): 4910–4911

74 Facchetti A. Electroactive oligothiophenes and polythiophenes for organic field effect transistors. *Handbook of Thiophene-Based Materials: Applications in Organic Electronics and Photonics*, 2009, 1: 595–646

75 Lu K, Liu Y. Polythiophenes: Important conjugated semiconducting polymers for organic field-effect transistors. *Curr Org Chem*, 2010, 14: 2017–2033

76 Gigli G, Barbarella G, Favaretto L, Cacialli F, Cingolani R. High-efficiency oligothiopene-based light-emitting diodes. *Appl Phys Lett*, 1999, 75: 439–441

77 Amb CM, Dyer AL, Reynolds JR. Navigating the color palette of solution-processable electrochromic polymers. *Chem Mater*, 2011, 23: 397–415

78 Gunbas G, Toppare L. Electrochromic conjugated polyheterocycles and derivatives–highlights from the last decade towards realization of long lived aspirations. *Chem Commun*, 2012, 48: 1083–1101

79 Bench R, Duflos J, Dupas G, Bourguignon J, Queguiner G. Synthesis and study of chiral nadh models in the thieno[2,3-b]pyridine series. *J Heterocycl Chem*, 1989, 26(6): 1595–1600

80 Chirakadze GG, Geliashvili EE, Gagolishvili MS. Synthesis and properties of thiophene containing azo dyes and pigments. *Izv Akad Nauk Gruz, Ser Khim*, 1999, 25: 203–209

81 Ivanova VN. Nitrogenous compounds of phenylated derivatives of thiophene. I. *Zh Obshch Khim*, 1958, 28: 1232–1238

82 Puterova Z, Krutošíková A, Végh D. Gewald reaction: Synthesis, properties and applications of substituted 2-aminothiophenes. *ARKIVOC*, 2010, i: 209–246

83 Buchstaller H-P, Siebert CD, Lyssy RH, Frank I, Duran A, Gottschlich R, Noe CR. Synthesis of novel 2-aminothiophene-3-carboxylates by variations of the gewald reaction. *Monats Chem*, 2001, 132(2): 279–293

84 Sabnis RW, Rangnekar DW, Sonawane ND. 2-Aminothiophenes by the gewald reaction. *J Heterocycl Chem*, 1999, 36(2): 333–345

85 Bourgeaux M, Vomscheid S, Skene WG. Optimized synthesis and simple purification of 2,5-diaminothiophene-3,4-dicarboxylic acid diethyl ester. *Synth Commun*, 2007, 37: 3551–3558

86 Gewald K. Heterocycles from ch-acidic nitriles. Vii. 2-Aminothiophene from a-oxo mercaptans and methylene-active nitriles. *Chem Ber*, 1965, 98(11): 3571–3577

87 Gewald K. Methods for the synthesis of 2-aminothiophenes and their reactions (review). *Chem Hetero Comp*, 1976, 12(10): 1077–1090

88 Gewald K, Gruner M, Hain U, Süptitz G. Zur ringumwandlung von 2-amino-thiophen-3-carbonsäureestern: Pyridon-und pyridazinon-derivate. *Monats Chem*, 1988, 119(8-9): 985–992

89 Gewald VK, Kleinert M, Thiele B, Hentschel M. Zur basenkatalysierten reaktion von methylenaktiven nitrilen mit schwefel. *J Prak Chem*, 1972, 314(2): 303–314

90 Angell RM, Atkinson FL, Brown MJ, Chuang TT, Christopher JA, Cichy-Knight M, Dunn AK, Hightower KE, Malkakorpi S, Musgrave JR, Neu M, Rowland P, Shea RL, Smith JL, Somers DO, Thomas SA, Thompson G, Wang R. *N*-(3-cyano-4,5,6,7-tetrahydro-1-benzothien-2-yl)amides as potent, selective, inhibitors of jnk2 and jnk3. *Bioorg Med Chem Lett*, 2007, 17: 1296–1301

91 Bowers S, Truong AP, Neitz RJ, Neitzel M, Probst GD, Hom RK, Peterson B, Galemmo RA, Jr., Konradi AW, Sham HL, Toth G, Pan H, Yao N, Artis DR, Brigham EF, Quinn KP, Sauer JM, Powell K, Ruslim L, Ren Z, Bard F, Yednock TA, Griswold-Prenner I. Design and synthesis of a novel, orally active, brain penetrant, tri-substituted thiophene based jnk inhibitor. *Bioorg Med Chem Lett*, 2011, 21: 1838–1843

92 De SK, Barile E, Chen V, Stebbins JL, Cellitti JF, Machleidt T, Carlson CB, Yang L, Dahl R, Pellecchia M. Design, synthesis, and structure-activity relationship studies of thiophene-3-carboxamide derivatives as dual inhibitors of the c-jun n-terminal kinase. *Bioorg Med Chem*, 2011, 19: 2582–2588

93 Grembecka J, He S, Shi A, Purohit T, Muntean AG, Sorenson RJ, Showalter HD, Murai MJ, Belcher AM, Hartley T, Hess JL, Cierpicki T. Menin-mll inhibitors reverse oncogenic activity of mll fusion proteins in leukemia. *Nat Chem Biol*, 2012, 8: 277–284

94 Aurelio L, Christopoulos A, Flynn BL, Scammells PJ, Sexton PM, Valant C. The synthesis and biological evaluation of 2-amino-4,5,6,7,8,9-hexahydrocycloocta[b]thiophenes as allosteric modulators of the a1 adenosine receptor. *Bioorg Med Chem Lett*, 2011, 21: 3704–3707

95 Kumar V, Madan AK. Prediction of the agonist allosteric enhancer activity of thiophenes with respect to human a1 adenosine receptors using topological indices. *Pharm Chem J*, 2007, 41: 140–145

96 Nikolakopoulos G, Figler H, Linden J, Scammells PJ. 2-Aminothiophene-3-carboxylates and carboxamides as adenosine a1 receptor allosteric enhancers. *Bioorg Med Chem*, 2006, 14: 2358–2365

97 Gaber HM, Bagley MC, Sherif SM. Antimicrobial investigations on synthetic p-tolylazo derivatives of thienopyrimidinone based on an ortho-functionalized thiophene nucleus. *Eur J Chem*, 2010, 1: 115–123

98 Panchamukhi SI, Mulla JAS, Shetty NS, Khazi MIA, Khan AY, Kalashetti MB, Khazi IAM. Benzothieno[3,2-e][1,2,4]triazolo [4,3-c]pyrimidines: Synthesis, characterization, antimicrobial activity, and incorporation into solid lipid nanoparticles. *Arch Pharm (Weinheim, Ger)*, 2011, 344: 358–365

99 Shams HZ, Mohareb RM, Helal MH, Mahmoud AE-S. Design and synthesis of novel antimicrobial acyclic and heterocyclic dyes and their precursors for dyeing and/or textile finishing based on 2-n-acylamino-4,5,6,7-tetrahydro-benzo[b]thiophene systems. *Molecules*, 2011, 16: 6271–6305

100 Hallas G, Choi JH. Synthesis and spectral properties of azo dyes derived from 2-aminothiophenes and 2-aminothiazoles. *Dyes Pigm*,

1999, 42(3): 249–265
101 Hallas G, Choi JH. Synthesis and properties of novel aziridinyl azo dyes from 2-aminothiophenes—Part 1: Synthesis and spectral properties. *Dyes Pigm*, 1999, 40(2-3): 99–117
102 Hallas G, Choi JH. Synthesis and properties of novel aziridinyl azo dyes from 2-aminothiophenes—Part 2: Application of some disperse dyes to polyester fibres. *Dyes Pigm*, 1999, 40(2-3): 119–129
103 Hallas G, Towns AD. Dyes derived from aminothiophenes. Part 1: Synthesis of some heterocyclic disperse dyes using the gewald reaction. *Dyes Pigm*, 1996, 32(3): 135–149
104 Hallas G, Towns AD. A comparison of the properties of some 2-aminothiophene-derived disperse dyes. *Dyes Pigm*, 1996, 31(4): 273–289
105 Hallas G, Towns AD. Dyes derived from aminothiophenes. Part 4: Synthesis of some nitro-substituted thiophene-based azo disperse dyes. *Dyes Pigm*, 1997, 33(4): 319–336
106 Hallas G, Towns AD. Dyes derived from aminothiophenes–Part 2. Spectroscepic properties of some disperse dyes derived from 2-aminothiophenes. *Dyes Pigm*, 1997, 33(3): 205–213
107 Hallas G, Towns AD. Dyes derived from aminothiophenes. Part 6: Application of some nitro-substituted thiophene-based azo disperse dyes to hydrophobic fibres. *Dyes Pigm*, 1997, 35(1): 45–55
108 Hallas G, Towns AD. Dyes derived from aminothiophenes—Part 3. Application of some disperse dyes derived from 2-aminothiophenes to hydrophobic fibres. *Dyes Pigm*, 1997, 33(3): 215–228
109 El-Shekeil A, Abu-Bakr AO. Dc electrical conductivity of the direct electrochemically synthesized polythiophene metal complexes. *J Macromol Sci Part A: Pure Appl Chem*, 2011, 48: 233–240
110 El-Shekeil A, Al-Khader M, Abu-Bakr AO. Synthesis, characterization and dc electrical conductivity of some oligmer mixed metal complexes. *Synth Met*, 2004, 143(2): 147–152
111 El-Dossoki FI. Electric conductance and semi-empirical studies on two thiophene derivatives/metal cation complexation. *J Mol Liq*, 2008, 142: 53–56
112 Skene WG, Dufresne S, Trefz T, Simard M. (e)-Diethyl 2-amino-5-(2-thienylmethyleneamino)thiophene-3,4-dicarboxylate. Acta Crystallogr, Sect E: Struct Rep Online, 2006, 62(6): o2382–o2384
113 Dufresne S, Bourgeaux M, Skene WG. Diethyl 2,5-bis((e)-thiophen-2-ylmethyleneamino)thiophene-3,4-dicarboxylate triad. Acta Crystallogr, Sect E: Struct Rep Online, 2006, 62(12): o5602–o5604
114 Wong BM, Cordaro JG. Electronic properties of vinylene-linked heterocyclic conducting polymers: Predictive design and rational guidance from dft calculations. *J Phys Chem C*, 2011, 115(37): 18333–18341
115 Qing F, Sun Y, Wang X, Li N, Li Y, Li X, Wang H. A novel poly(thienylenevinylene) derivative for application in polymer solar cells. *Polym Chem*, 2011, 2(9): 2102–2106
116 Gergely J, Morgan JB, Overman LE. Stereocontrolled synthesis of functionalized cis-cyclopentapyrazolidines by 1,3-dipolar cycloaddition reactions of azomethine imines. *J Org Chem*, 2006, 71: 9144–9152
117 Bourgeaux M, Skene WG. Photophysics and electrochemistry of conjugated oligothiophenes prepared by using azomethine connections. *J Org Chem*, 2007, 72(23): 8882–8892
118 Guarìn SAP, Bourgeaux M, Dufresne S, Skene WG. Photophysical, crystallographic, and electrochemical characterization of symmetric and unsymmetric self-assembled conjugated thiopheno azomethines. *J Org Chem*, 2007, 72(7): 2631–2643
119 Mielke J, Leyssner F, Koch M, Meyer S, Luo Y, Selvanathan S, Haag R, Tegeder P, Grill L. Imine derivatives on Au(111): Evidence for "inverted" thermal isomerization. *ACS Nano*, 2011, 5(3): 2090–2097
120 Luo Y, Utecht M, Dokić J, Korchak S, Vieth H-M, Haag R, Saalfrank P. *Cis-trans* isomerisation of substituted aromatic imines: A comparative experimental and theoretical study. *ChemPhysChem*, 2011, 2311–2321
121 Traven' V, Ivanov I, Panov A, Safronova O, Chibisova T. Solvent-induced E/Z (C=N)-isomerization of imines of some hydroxy-substituted formylcoumarins. *Rus Chem Bull*, 2008, 57(9): 1989–1995
122 Selli E. Photochemistry of n-benzylideneanilinium cations in concentrated sulfuric acid solutions. *J Photochem Photobiol A*, 1996, 101(2-3): 185–188
123 Geissler G, Fust W, Krüger B, Tomaschewski G. Azomethinimine. Vii. Photochemisches und thermisches verhalten azarylsubstituierter pyrazolidon-(3)-azomethinimine. *J Prak Chem*, 1983, 325(2): 205–210
124 Russegger P. Photoisomerization about carbon—nitrogen double bonds. I. Kinetic and potential energy for ground and excited states of methylenimine. *Chem Phys*, 1978, 34(3): 329–339
125 Traven VF, Miroshnikov VS, Pavlov AS, Ivanov IV, Panov AV, Chibisova TyA. Unusual e/z-isomerization of 7-hydroxy-4-methyl-8-[(9h-fluoren-2-ylimino)methyl]-2h-1-benzopyran-2-one in acetonitrile. *Mendeleev Commun*, 17(2): 88–89
126 Dufresne S, Skene WG. Optoelectronic property tailoring of conjugated heterocyclic azomethines—the effect of pyrrole, thiophene and furans. *J Phys Org Chem*, 2011, 211–221
127 Roncali J. Conjugated poly(thiophenes): Synthesis, functionalization, and applications. *Chem Rev*, 1992, 92(4): 711–738
128 Lee CK, Yu JS, Lee HJ. Determination of aromaticity indices of thiophene and furan by nuclear magnetic resonance spectroscopic analysis of their phenyl esters. *J Heterocyclic Chem*, 2002, 39(6): 1207–1217
129 Dufresne S, Bolduc A, Skene WG. Towards materials with reversible oxidation and tuneable colours using heterocyclic conjugated azomethines. *J Mater Chem*, 2010, 20(23): 4861–4866
130 Bolduc A, Dufresne S, Skene WG. Edot-containing azomethine: An easily prepared electrochromically active material with tuneable colours. *J Mater Chem*, 2010, 20(23): 4820–4826
131 Dong Y, Navarathne D, Bolduc A, McGregor N, Skene WG. *A,α′*-n-boc-substituted bi- and terthiophenes: Fluorescent precursors for functional materials. *J Org Chem*, 2012, 77(22): 5429–5433
132 Lakowicz JR. *Principles of Fluorescence Spectroscopy*. New York: Springer, 2006
133 Bourgeaux M, Guarin SAP, Skene WG. Photophysical, crystallographic, and electrochemical characterization of novel conjugated thiopheno azomethines. *J Mater Chem*, 2007, 17(10): 972–979
134 Luo Y, Korchak S, Vieth HM, Haag R. Effective reversible photoinduced switching of self-assembled monolayers of functional imines on gold nanoparticles. *Chem Phys Chem*, 2011, 12(1): 132–135
135 Bléger D, Ciesielski A, Samorì P, Hecht S. Photoswitching vertically oriented azobenzene self-assembled monolayers at the solid–liquid interface. *Chem Eur J*, 2010, 16(48): 14256–14260
136 Bourque AN, Dufresne S, Skene WG. Conjugated fluorenes prepared from azomethines connections: The effect of alternating fluorenones and fluorenes on the spectroscopic and electrochemical properties. *J Phys Chem C*, 2009, 113(45): 19677–19685
137 Dufresne S, Skalski T, Skene WG. Insights into the effect of ketylimine, aldimine, and vinylene group attachment and regiosubstitution on the fluorescence deactivation of fluorene. *Can J Chem*, 2011, 89(2): 173–180
138 Dufresne S, Roche IU, Skalski T, Skene WG. Insights into the effect of the ketylimine group on the fluorescence deactivation of oligofluorenes. *J Phys Chem C*, 2010, 114(30): 13106–13112
139 Dufresne S, Bourque AN, Skene WG. (e)-5-(2-Thienylmethylen-eamino)quinolin-8-ol. *Acta Crystallogr, Sect E: Struct Rep Online*, 2008, 64(1): o316
140 Skene WG, Dufresne S, Trefz T, Simard M. (e)-Diethyl 2-amino-5-(2-thienylmethyleneamino)thiophene-3,4-dicarboxylate. *Acta Crystallogr, Sect E: Struct Rep Online*, 2006, E62(6): o2382–o2384
141 Dufresne S, Bourgeaux M, Skene WG. Diethyl 2,5-bis[(e)-thiophen-2-ylmethyleneamino]thiophene-3,4-dicarboxylate. *Acta Crystallogr, Sect E: Struct Rep Online*, 2006, 62(12): o5602–o5604
142 Dufresne S, Skene WG. Diethyl 2,5-bis[(1e)-(1h-pyrrol-2-ylmethylidene)amino]thiophene-3,4-dicarboxylate. *Acta Crystallogr, Sect E: Struct Rep Online*, 2011, 67(9): o2302
143 Dufresne S, Skene WG. Diethyl 2-amino-5-[(e)-(1-methyl-

1h-pyrrol-2-yl)methylideneamino]thiophene-3,4-dicarboxylate. *Acta Crystallogr, Sect E: Struct Rep Online*, 2010, 66(12): o3221
144 Dufresne S, Skene WG. Diethyl 2-amino-5-[(e)-(furan-2-ylmethylidene)amino]thiophene-3,4-dicarboxylate. *Acta Crystallogr, Sect E: Struct Rep Online*, 2010, 66(11): o3027
145 Dufresne S, Skene WG. Diethyl 2-[(1-methyl-1h-pyrrol-2-yl)methyleneamino]-5-(2-thienylmethyleneamino)thiophene-3,4-dicarboxylate. *Acta Crystallogr, Sect E: Struct Rep Online*, 2008, 64(5): o782
146 Dufresne S, Skene WG. Diethyl 2,5-bis[(e)-2-furylmethyleneamino]thiophene-3,4-dicarboxylate. *Acta Crystallogr, Sect E: Struct Rep Online*, 2008, 64(4): o710
147 Dufresne S, Bolduc A, Skene WG. Diethyl 2,5-bis[(2,3-dihydrothieno[3,4-b][1,4]dioxin-5-yl)methylideneamino]thiophene-3,4-dicarboxylate acetone monosolvate. *Acta Crystallogr, Sect E: Struct Rep Online*, 2011, 67(12): o3138
148 Bourgeaux M, Vomsheid S, Skene WG. Hydrogen-bonded network of diethyl 2,5-diaminothiophene-3,4-dicarboxylate. *Acta Crystallogr, Sect E: Struct Rep Online*, 2006, 62(12): o5529–o5531
149 Ruban G, Zobel D. Crystal structure of *trans*-1,2-di-2-thienylethene. *Acta Crystallogr, Sect B*, 1975, B31: 2632–2634
150 Dogan F, Kaya I, Bilici A. Azomethine-based phenol polymer: Synthesis, characterization and thermal study. *Synth Met*, 2011, 161(1-2): 79–86
151 El-Shekeil AG, Al-Yusufy FA, Saknidy S. Dc conductivity of some polyazomethines. *Polym Int*, 1997, 42(1): 39–44
152 Iwan A, Sek D. Processible polyazomethines and polyketanils: From aerospace to light-emitting diodes and other advanced applications. *Prog Polym Sci*, 2008, 33(3): 289–345
153 Bourgeaux M, Skene WG. A highly conjugated p- and n-type polythiophenoazomethine: Synthesis, spectroscopic, and electrochemical investigation. *Macromolecules*, 2007, 40(6): 1792–1795
154 Hall HKJ, Padias AB, Williams PA, Gosau JM, Boone HW, Park DK. Novel polyaromatic quinone imines. *Macromolecules*, 1995, 28(1): 1–8
155 Bourgeaux M, Skene WG. A highly conjugated p- and n-type polythiophenoazomethine: Synthesis, spectroscopic, and electrochemical investigation. *Macromolecules*, 2007, 40(6): 1792–1795
156 Giuseppone N. Toward self-constructing materials: A systems chemistry approach. *Acc Chem Res*, 2012, DOI: 10.1021/ar2002655
157 Rue NM, Sun J, Warmuth R. Polyimine container molecules and nanocapsules. *Israel J Chem*, 2011, 51(7): 743–768
158 Ciesielski A, Samori P. Supramolecular assembly/reassembly processes: Molecular motors and dynamers operating at surfaces. *Nanoscale*, 2011, 3(4): 1397–1410
159 Lehn J. Dynamers: Dynamic molecular and supramolecular polymers. *Aust J Chem*, 2010, 63(4): 611–623
160 Meyer CD, Joiner CS, Stoddart JF. Template-directed synthesis employing reversible imine bond formation. *Chem Soc Rev*, 2007, 36(11): 1705–1723
161 Barik S, Bishop S, Skene WG. Spectroelectrochemical and electrochemical investigation of a highly conjugated all-thiophene polyazomethine. *Mater Chem Phys*, 2011, 129(1-2): 529–533
162 Ryan B, McCann G. Novel sub-ceiling temperature rapid depolymerization-repolymerization reactions of cyanoacrylate polymers. *Macromol Rapid Commun*, 1996, 17: 217–227
163 Wong BM, Cordaro JG. Electronic properties of vinylene-linked heterocyclic conducting polymers: Predictive design and rational guidance from dft calculations. *J Phys Chem C*, 2011, 115(37): 18333–18341
164 Bentkowska H. The effect of factors breaking the siloxane bond on the repolymerization course of siloxanes. I. Effect of hydrogen chloride on cyclic and linear poly(diethylsiloxane). *Rocz Chem*, 1963, 37: 717–721
165 Barik S, Skene WG. Selective chain-end postpolymerization reactions and property tuning of a highly conjugated and all-thiophene polyazomethine. *Macromolecules*, 2010, 43(24): 10435–10441

After completing her B.Sc. degree in Chemistry at the Université de Montréal, BOLDUC Andréanne (left) joined Skene's group as a M. Sc. student in 2008 and then transferred directly into the Ph.D. program. Her thesis focusses on preparing and examining new conjugated azomethines for different plastic electronic applications. MALLET Charlotte (center) completed her Ph.D. studies in 2010 at the Universitéd'Angers, France. She joined Skene's group as a postdoctoral fellow in 2011, where she works on conjugated benzothiadiazole derivatives for fluorescence applications. SKENE William (right) is an associate professor at U de M. His research interests are the design, synthesis, and characterization of easily prepared conjugated materials for plastic electronics and the structure-property studies of these materials.